Recent developments in DNS of turbulent combustion

Pascale Domingo, Luc Vervisch

Recent developments in DNS of Turbulent Combustion

Pascale Domingo and Luc Vervisch
CORIA - CNRS and INSA Rouen Normandie, Technopole du Madrillet, BP 8
76801 Saint-Etienne-du-Rouvray, France

Abstract

The simulation of turbulent flames fully resolving the smallest flow scales and the thinnest reaction zones goes along with specific requirements, which are discussed from dimensionless numbers useful to introduce the generic context in which direct numerical simulation (DNS) of turbulent flames is performed. Starting from this basis, the evolution of the DNS landscape over the past five years is reviewed. It is found that the flow geometries, the focus of the studies and the overall motivations for performing DNS have broadened, making DNS a standard tool in numerical turbulent combustion. Along these lines, the emerging DNS of laboratory burners for turbulent flame modeling development is discussed and illustrated from DNS imbedded in Large Eddy Simulation (LES) and flow resolved simulation of bluff-body flames. The literature shows that DNS generated databases constitute a fantastic playground for developing and testing a large spectrum of promising machine learning methods for the control and the optimisation of combustion systems, including novel numerical approaches based on the training of neural networks and which can be evaluated in DNS free from sub-model artefacts. The so-called quasi-DNS is also progressively entering the optimisation loop of combustion systems, with the application of techniques to downsize real combustion devices in order to perform fully resolved simulations of their complex geometries. An example of such study leading to the improvement of an incinerator efficiency is reported. Finally, numbers are given relative to the carbon footprint of the generation of DNS databases, motivating the crucial need for community building around database sharing.

Keywords: Flame, Turbulent Combustion; Direct Numerical Simulation; Sub-grid scale modeling

1. Introduction

The concept of Direct Numerical Simulation (DNS) was first introduced by Orszag back in the 70's [1]. The objective at that time was to access emerging theories on flow turbulence from fully resolved space and time solutions of the first principle equations describing incompressible, isotropic and homogeneous turbulence. Early in the 80's, DNS was extended to scalar transport [2, 3] considering various shear flows, such as turbulent mixing layers and wall bounded flows. DNS then became a useful tool to discuss and to calibrate numerical models in view of their application to flows of engineering interest [4].

Chemical reactions were introduced in constant density DNS during the same period [5–7]. The gap to reach direct numerical simulation of combustion and flames was closed in the early 90's by accounting for all the effects induced by heat release and variable density, first with global chemical schemes [8–10] and then including detailed chemistry [11]. Carrier phase DNS, in which the flow is fully resolved only in the far field of liquid or solid fuels represented by lagrangian source points, was introduced right after for fuel spray [12–14] and more recently for solid fuel combustion [15].

Since the 90's, the archival literature on combustion DNS has flourished; this paper focusses on the most recent years, i.e., between 2017 and 2022.

Combustion DNS can be classified in terms of the level of complexity retained for both, the description of the reacting flow physics and the geometry of the problem considered. Thermodynamics and momentum are fully coupled in compressible DNS and weakly coupled in the variable density low Mach number framework [16]. Simple or complex multicomponent molecular-transport properties [17] have been used in both formulations, the same for chemistry from single-step up to fully detailed mechanisms [18]. Adaptive mesh refinement also played a key role in the progress of DNS [19, 20]. The most advanced DNS have considered laboratory flames with high-order fully compressible numerics [21] (Fig. 1).

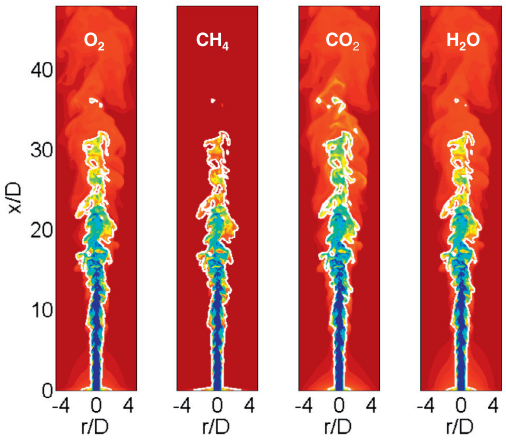

Fig. 1: Progress variable distribution based on different definitions in DNS of a high Karlovitz CH4/Air premixed jet flame. Reprinted with permission [21].

Originally, specific spectral numerical methods were developed to secure the simulation of turbulence free from numerical artefact [22]. Spectral methods implies periodic boundary conditions and constant density fluid. Thereby to tackle canonical problems more representative of turbulent flames, the use of compact discretizations with spectral like resolution [23] and able to handle all kinds of boundary conditions [24–26] became popular in combustion DNS. Still, these numerical schemes are difficult to apply away from geometries involving simplified free shear flows (Fig. 2 and 3). With the rapid progress in computing power and the availability of numerous multicomponent low-order accurate finite-volume flow solvers, simulations of laboratory burners attempting to fully resolve the smallest velocity and scalar scales have emerged. Because most numerical methods do not exactly secure the correct turbulent kinetic energy transfer between the largest and the smallest scales, these simulations are sometimes called, quasi-DNS or flame resolved-DNS [27]. Quasi-DNS was defined in [28] as 'a model-free simulation which does not fulfill all of the strict requirements of a DNS, e.g. for complex geometries which do not allow the use of higher order discretization schemes, but is accurate enough so that the results of a full DNS are expected to be similar'. (In the first occurrence of quasi-DNS back twenty years ago [29], the resolution was below twice the Kolmogorov scale.) The effect of spurious numerical dissipation in such quasi-DNS needs to be carefully calibrated [30]. The wording flame resolved-DNS indicates that no compromise is present on the description of the flame structure. Interestingly, these simulations have been found valuable because they allow to bridge between the investigation of turbulent flames in the lab and on the computer. Going further along these lines, after performing proper rescaling of the physical parameters at play, quasi-DNS of downsized real geometries of reactive flow systems have been reported and exploited for furnace design [31].

Ultimately, it is likely that finite-volume high-order spectral element based methods [34], now widely applied to DNS of non-reacting and reacting flows [35, 36], will become a standard to perform numerically reliable fully resolved simulations in geometries featuring many properties of real combustion systems.

DNS is motivated by a variety of quests in combustion science. The objective of evaluating the prediction capabilities of turbulent combustion models for Reynolds Averaged Navier-Stokes (RANS) calculations or Large Eddy Simulation (LES) is usually put forward. DNS is indeed an ideal test-bed for assessing modeling hypotheses, specifically because DNS in canonical configurations enables extensive parametric studies. In practice, not all the closures directly is-

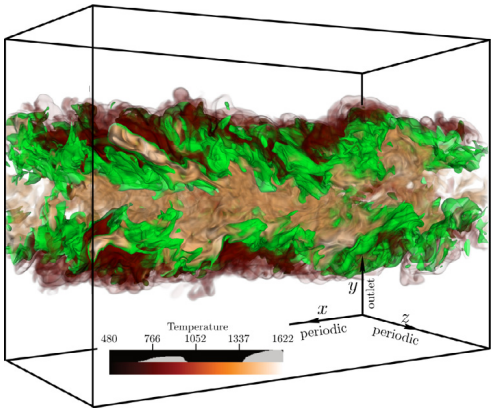

Fig. 2: Three-dimensional direct numerical simulations of temporally evolving turbulent H2 jet flames. Green: Stoichiometric iso-surface. Contour: Temperature. Reprinted with permission [32].

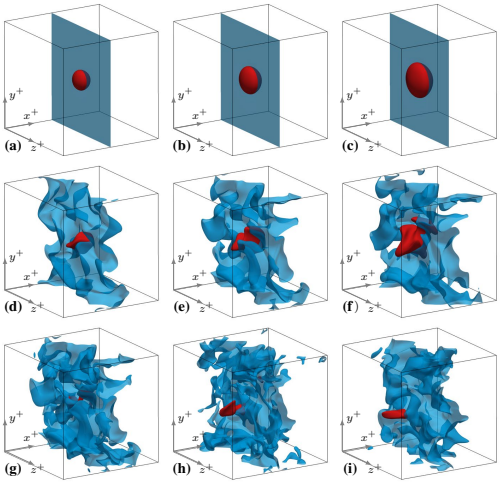

Fig. 3: Time evolution of an igniting kernel in isotropic turbulence, study of the effect of biogas compositon. Blue: Stoichiometric iso-surface. Red: Temperature (60% of max level). Reprinted with permission [33].

sued from DNS databases have found their way in engineering software. This may be partially the result of the low-Reynolds number character of many of these simulations. In practice, the turbulence integral length scale is of the order of the flame thickness in DNS, so missing part of the multi-scale flame/turbulence interactions. Also the so-called a-priori tests, where models are tested from exact (DNS) and frozen values of their input parameters, cannot always allow for reaching definitive conclusions, because is missing the potential error accumulation and error compensation existing when iterating the statistical models over time.

In fact, it is in the analysis of the detail of the flame physics that DNS has been the most successful, specifically when those details cannot be reached by the most advanced experimental tools. The behaviors of thermochemical quantities and scalars in flames [37–39] and constitutive relations to calibrate different flame dynamics [40–43], can easily be identified from DNS. In short, DNS has been shown to be a valuable tool when the roadmap is driven by clear reacting flow physics stumbling block needed clarifications, as shown in recent reviews on the subject [18, 44–48].

The number of published gaseous flame DNS articles in the combustion journals grew linearly (of about 80 between 2007-2011, 140 between 2012-2016 and 200 between 2017-2021). They have been devoted to fully premixed flames [21, 27, 37, 38, 41–43, 49–75, 75–190], non-premixed and multi-regimes combustion [32, 46, 191–219]. The high Karlovitz regime benefits from a growing interest [21, 37, 38, 41–43, 50, 60, 67, 69, 82, 103, 104, 106, 141, 144, 154, 162, 167, 170, 174, 186, 187, 190, 220]. Some of these simulations are with single- or two-step global chemistry [76, 85, 87, 93, 99, 103, 112, 115, 128, 129, 144, 145, 161, 221]. The chemistry of methane has motivated many works [21, 27, 41, 42, 50, 52, 54, 56, 61, 62, 68, 74, 77, 82, 84, 88–90, 92, 93, 96, 97, 101, 103, 107, 110, 113, 114, 118, 119, 123, 133, 134, 138, 145, 155, 156, 163, 169, 176, 182, 184, 189, 207, 211, 217, 220, 222, 223], also hydrogen [32, 38, 43, 60, 69, 70, 78, 79, 81, 90, 95, 97–99, 102, 105, 106, 109, 117, 120, 124, 126, 127, 129, 132, 136, 154, 160, 171, 172, 174, 181–183, 185, 193, 195, 204, 209, 214, 218, 224–229], heavy fuel [37, 38, 53, 66, 88, 100, 108, 140, 145, 151, 162, 170, 180, 197, 203, 221, 230–232], syngas [66, 114, 166, 181, 212, 215, 216] and very recently ammonia [97]. Models were discussed from DNS within RANS [64, 112, 113, 128, 189, 233] and LES context [32, 37, 46, 51, 65, 67, 77, 94, 103, 112, 119, 123, 140, 143, 149, 157, 163, 164, 166, 167, 169, 173, 179, 187, 190, 193, 195, 197, 203, 210, 212, 213, 221, 222, 233–237]. Finally, DNS for machine learning related method is rapidly emerging [51, 110, 139, 140, 146, 173, 175, 186, 215, 216, 222, 234].

These works have been produced using DNS softwares which are lab-developped or community codes often shared between different teams worldwide, such as SENGA [238], S3D [239], DINO [240], FK^3 [241], KARFS [242], PsiPhi [243], HOLOMAC [244], NGA [245], AVBP [246], Nek5000 [247] or OpenFoam [248]. Some of these codes are either high-order accurate in space, ranging from 6th to 10th order (SENGA, DINO, S3D, FK^3, KARFS, HOLOMAC), Nek5000 (spectral elements), or 4th or even 2nd order (NGA, PsiPhi, AVBP, OpenFoam).

The paper is organised as followed. The resolution requirements for DNS are discussed first. Then, two recent DNS of laboratory burners, based either on an DNS imbedded in LES approach or on a full resolution of the turbulent flame, are presented. These DNS configurations are of interest because they have been complemented by a-posteriori LES studies. Af-

ter that, the role of DNS as one of the ingredient in the development of machine learning for combustion simulation is addressed. Given the limitations of DNS already discussed, an alternative approach to canonical geometries is discussed, which is based on the downsizing of real combustion system geometries. Its application to selective non-catalytic reduction of nitric oxides is shown, with an exemple of improvement of a real industrial furnace from DNS. Before concluding, the cost of DNS is examined in the light of its carbon footprint.

2. Resolution requirements for combustion DNS

DNS meshes are calibrated to secure the full resolution of the smallest turbulent flow scales and of the thinnest reaction zones. The strength of the turbulence is characterised by the turbulent Reynolds number

$$Re_T = \frac{k^{1/2}\ell_T}{\nu} \approx \left(\frac{\ell_T}{\eta_k}\right)^{4/3} , \qquad (1)$$

where ν is the kinematic viscosity of the gas, $\langle\rho\rangle\, k = 0.5\,\langle\rho u_i u_i\rangle - 0.5\,\langle\rho u_i\rangle\,\langle\rho u_i\rangle\,/\,\langle\rho\rangle$ is the turbulent kinetic energy per unit of volume, where $\langle\,\cdot\,\rangle$ denotes Reynolds averaging. ρ is the density, ℓ_T is the integral length scale of the fluctuating field and η_k is the Kolmogorov characteristic length of the smallest dissipative eddies. It was demonstrated that a mesh resolutions of $h = 2\eta_k$ is sufficient for capturing the dissipative range [249]. For simulating a three-dimensional turbulence covering a volume $V = L_o^3$, the number of grid points scales as

$$N = \left(\frac{L_o}{2\eta_k}\right)^3 = \left(\frac{L_o}{2\ell_T}\right)^3 Re_T^{9/4} . \qquad (2)$$

Re_T in a representative swirl burner gas turbine is of the order of 1500, with an integral length scale of the order of 5 mm [250]. Then, to resolve 10^3 cm^3 of shear layer, more than 10 billon mesh points are required.

The reaction zone brings additional length and time scales associated to the Damköhler and the Karlovitz numbers,

$$Da = \frac{\tau_T}{\tau_c} \approx \frac{1}{\tau_c}\frac{k}{\epsilon} , \qquad (3)$$

$$Ka = \frac{\tau_c}{\tau_k} \approx \tau_c \left(\frac{\epsilon}{\nu}\right)^{1/2} , \qquad (4)$$

$$Da \times Ka \approx Re_T^{1/2} , \qquad (5)$$

where τ_c is an estimation of the chemical time, τ_T is the integral turbulent time and τ_k is the small-scale (Kolmogorov) turbulence time scale.

In terms of mesh requirement, (2) and (5) provide

$$N = \left(\frac{L_o}{2\ell_T}\right)^3 Da \times Ka \times Re_T^{7/4} . \qquad (6)$$

Major limitations of DNS emerge from this relation. To keep N at a practical level, the Damköhler, Karlovitz and turbulent Reynolds numbers cannot be simultaneously too large. In addition, the number L_o/ℓ_T of integral length scales that will be contained in the computational domain is also a limiting factor.

In canonical geometry DNS, such as planar flames interacting with homogeneous or shear turbulence [37, 136], it is usually Re_T that is put forward with $L_o \simeq \ell_T$, i.e., the computational domain spanning only a few integral length scales. These DNS are valuable to study the impact of small scales turbulence on the reaction zones, however with a very limited spectrum of flame wrinkling lengths.

In turbulent flames of the real world, according to the relation (5), at very high Reynolds numbers ($\mathrm{Re_T} \to \infty$), chemistry can still be fast ($\mathrm{Da} \to \infty$), as long as the chemical time scale is shorter than the shortest of the flow time scales, *i.e.* the amplitude of Ka stays moderate. It is usually believed that most practical combustion systems operate under this regime [251]. Equation (6) suggests that the exploration of high Da and Ka regimes by DNS is limited by the number of mesh cells which can be accommodated. For instance, at a fixed value of Da at which combustion occurs, $\mathrm{Re_T} \approx \mathrm{Ka}^2$ and increasing the Karlovitz number by a factor α would mean increasing the turbulent Reynolds number by a factor α^2, which cannot always be achieved because of the limitation brought by (6). In the practice of most DNS, when Ka increases, Da decreases or Re_T takes very moderate values.

These limitations all come down to $N \times n_{\mathrm{eq}}$, with n_{eq} the number of equations to be solved, which grows linearly with the number of chemical species included in the simulation. However, because detailed chemistry goes with an increased stiffness of the system, the CPU cost does not simply scale linearly with the number of species. DNS with simplified chemistry can then potentially reach higher Reynolds and Karlovitz numbers than those with fully detailed chemistry, or at least allow for a more systematic investigation of parameter ranges.

In the end, a compromise must be achieved between embarking into huge computing efforts, to approach realistic values of the turbulent combustion characteristic numbers, or providing more modest but databases easier to handle. Indeed, the literature shows that very large databases may be less successful than smaller ones in terms of number of research groups probing them for flow physics analysis or modeling development.

3. DNS of laboratory burners

3.1. DNS imbedded in LES

To limit the CPU cost necessary to simultaneously resolve the development of the turbulent shear layers driven by the velocity gradients at the largest scales, and, the downstream interaction of the flame with the velocity fluctuations, in many DNS synthetic velocity fluctuations are imposed to flames. The advantage is a careful control of the characteristic velocity

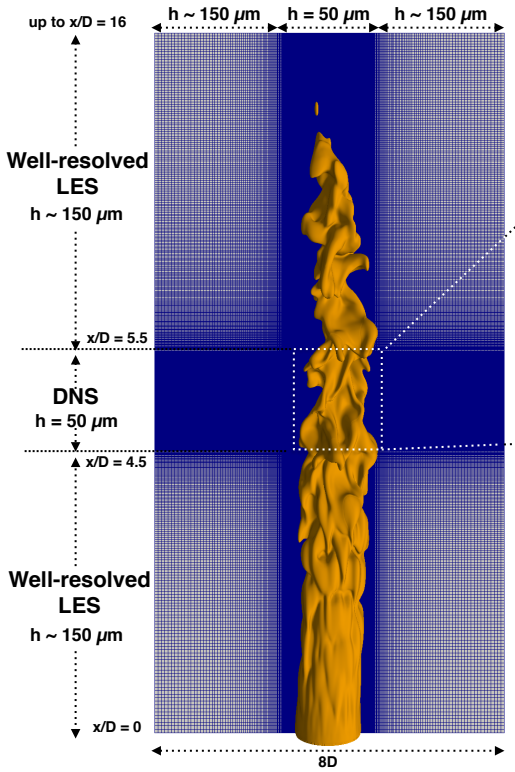

Reynolds	Nozzle diameter	Bulk velocity	Kinetic energy
24,000	12mm	30 m/s	3.82 m^2/s^2
U'/S_L (DNS ZONE)	**Karlovitz number** (DNS ZONE)	**Stoichiometric CH4/Air Fuel jet temperature**	**Burnt gases pilot temperature**
5	$3 < Ka < 5$	300K	2200K

Fig. 4: Three LES-DNS zones of the jet-flame simulation. Mesh and iso-progress variable $c = 0.8$. h denotes the mesh resolution. Reprinted with permission [252]

scales and of the energetic spectrum of the fluctuations. However, the evolutions in space and time of the velocity field seen by the flame may strongly differ from those observed in real burners.

DNS imbedded in LES was recently proposed to overcome this limitation [77], keeping the computing effort to a reasonable level (the same low dissipative numerical discretisation is used for both LES and DNS). The development of the rolling up of the shear layers in a jet flame is simulated from the burner exit applying well resolved LES, including sub-grid scale models for the flame and the flow. The resolution of this LES zone must be sufficient to resolve a significant part of the large-scale flame wrinkling. Then, at a given streamwise location, the mesh is refined over a distance which allows for the turbulence to develop, with the full spectrum of velocity and scalar scales resolved. The streamwise distance over which DNS is performed must be calibrated so that the turbulence/chemistry interaction has time to be fully established. In premixed flames, this can be done for instance using scaling laws derived from first principles for the dynamics of δ_T, the flame brush thickness [253]. Starting from $\delta_T(t_o)$ within a turbulence featuring ℓ_T and τ_T as turbulent integral length and time scales, respectively,

$$\begin{aligned}\delta_T^2(t) &\approx b_2^2 \ell_T^2 \left(1 - \exp(-C_s(t-t_o)/\tau_T)\right) \\ &+ \delta_T^2(t_o) \exp(-C_s(t-t_o)/\tau_T)\,, \end{aligned} \quad (7)$$

with $b_2 = 1.78$ [253]. Because $C_s \approx 2$ [254], the mean turbulent flame brush adjusts to turbulence with a characteristic time of the order of half the eddy turnover time ($b_2 = 1.78$). In the LES imbedded DNS shown in Fig. 4, the eddy turn over time is of the order of 1.13 ms at the start of the DNS zone for a residence time in the refined mesh of the order of 2 ms. This premixed jet-flame configuration retained was studied experimentally [255]. The bunsen burner features a nozzle diameter of D = 12 mm. The Reynolds number of the case considered is 24,000, corresponding to a mean nozzle velocity of 30 m/s and a level of turbulent kinetic energy of 3.82 m^2/s^2. The LES mesh contains about 171 million nodes covering a domain of 16D×8D×8D, with a resolution of the order of 150 μm. The embedded DNS box located at 4.5D from the nozzle contains 28.58 million nodes, covering a physical domain of 12mm×18mm×18mm, with a fixed resolution of 50μm. The flame thermal thickness estimated from the progress variable field is of the order of $\delta_L \approx 400\mu$m and the Kolmogorov scale reported from experiments is of the order of 50μm in this zone. Downstream of the DNS, the sim-

ulation resumes to LES. Chemistry is tabulated with premixed flamelet (GRI-3.0 mechanism [256] and progress variable [257]) for both LES and DNS. A presumed filtered density probability function [258] is used to account for the unresolved fluctuations of progress variable in the LES zones and the SGS momentum fluxes are modeled [259].

This database was explored first to elucidate the interlinks between scalar fields geometries at small-scales and the variable density flow dynamics, decomposed into four regions (fresh reactants/preheat/burning/hot products). The objective was to progress in micro-mixing modeling based on flow topologies [39, 260]. The prevalence of concave geometries towards the fresh reactants was reported in front of the burning region, while convex structures are more probable in the hot products.

Probing such DNS also promoted discussions

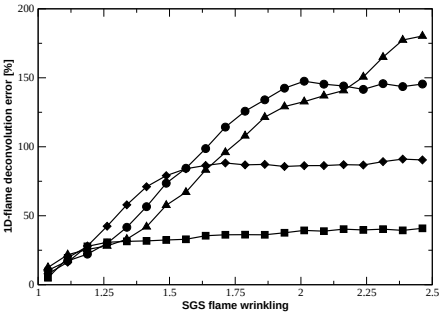

(a) $E(\Xi)$ in %

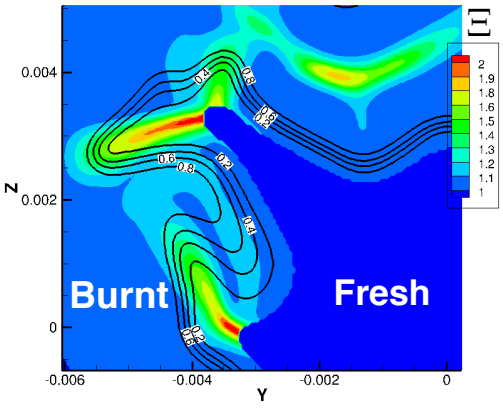

(b) $\Xi(\underline{x},t) = \overline{|\nabla\phi|}/|\nabla\overline{\phi}|$

Fig. 5: (a) Conditional mean on the subgrid flame wrinkling of the relative error on c between DNS and 1D-flamelet tabulated deconvolution, $E(\Xi)$, for various filter sizes. ■: Δ= 0.75 δ_L, ♦: 1.50 δ_L, ●: 2.25 δ_L, ▲: 3.00 δ_L. (b) snapshot of $\Xi(\underline{x},t)$ for Δ = 1.50 δ_L with DNS iso-c. Reprinted with permission [77].

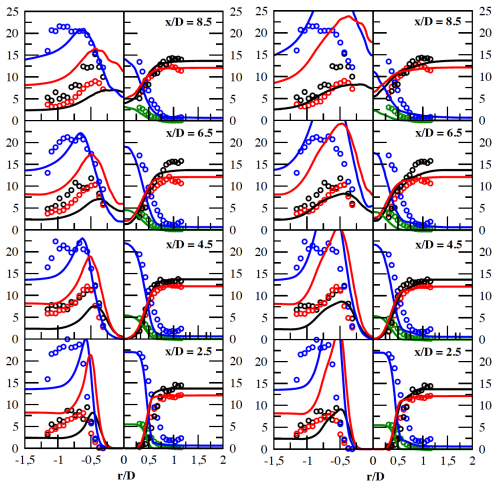

(a) 3D-deconvolution (b) 1D-Flame tabulated deconvolution

Fig. 6: Mass fractions in %. Symbol measurements [255]. Line: LES. In each subfigure: Left: Red: CO×10. Black: H_2×100. Blue: OH×75. Right: Blue: O_2. Green: CH_4. Red: H_2O. Black: CO_2. Reprinted with permission [77].

on the links between the well-established IEM (or EMST) [261] micro-mixing model

$$D_\phi \nabla^2 \phi(\underline{x},t) \approx \frac{\overline{\phi}(\underline{x},t) - \phi(\underline{x},t)}{\tau_T}\,, \qquad (8)$$

and its backward application to deconvolute (or 'unmix') the LES scalar field within the sub-grid scale with a characteristic time $\tau_T = \Delta^2/(24 D_\phi)$ (Δ is the LES filter size and D_c the molecular diffusion coefficient). This corresponds in fact to an implicit formulation of a truncated expansion of the Gaussian filter,

$$\phi(\underline{x},t) = \widetilde{\mathcal{L}}_\Delta^{-1}(\overline{\phi}) = \overline{\phi}(\underline{x},t) - \frac{\Delta^2}{24}\nabla^2\overline{\phi}(\underline{x},t)\,.$$

In LES sub-grid scale modeling, the approximated and deconvoluted scalar field can be used to compute the non-linear terms, which are then explicitly filtered to then advance the solution in time. Iterative deconvolution approaches and other based on the training of neural networks have also been discussed from other DNS flame configurations [262–266].

The conditional mean on the SGS flame wrinkling ($\Xi(\underline{x},t) = \overline{|\nabla c|}/|\nabla\overline{c}|$) of the normalised departure between the progress variable from DNS and its estimation from a one-dimensional flamelet tabulated deconvolution (see Fig. 7 for the test procedure) is shown in Figure 5 along with the distribution of $\Xi(\underline{x},t)$ for $\Delta = 1.50\delta_L$. As expected, the peak of SGS flame wrinkling occurs preferentially in the highly curved flame zones, while the error brought by 1D-flamelet deconvolution grows with Ξ. Interestingly, for every filter size ($0.75 < \Delta/\delta_L < 3$), there

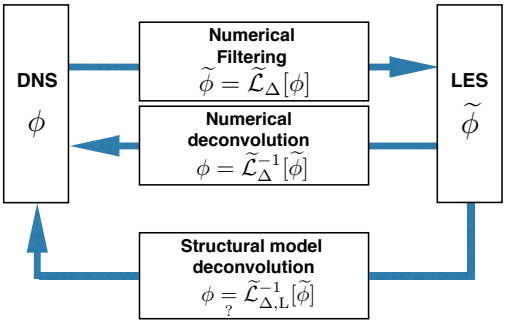

Fig. 7: Schematic of the filtering/deconvolution procedure. $\widetilde{\mathcal{L}}_\Delta^{-1}$: Inverse filtering deconvolution. $\widetilde{\mathcal{L}}_{\Delta,\mathrm{L}}^{-1}$: One-dimensional filtered flamelet deconvolution.

is a threshold value of Ξ, above which this error stays almost constant.

Such modeling concepts can be tested and immediately evaluated making the mesh coarser in the DNS zone to switch to LES ($170\mu\mathrm{m} < \Delta < 640\mu\mathrm{m}$). This allows for correlating the exact source of weaknesses of modeling, observed in a-priori tests, with the statistical results obtained applying the closures. Figure 6(b) displays the averaged results. Flamelet-based deconvolution indeed overestimates the consumptions of CH_4 and O_2, which is less pronounced in Fig. 6(a), with three-dimensional deconvolution [268]. The overestimation of CO is also enhanced with one-dimensional tabulated flame deconvolution.

This DNS embedded LES was also used to train convolutional neural networks to predict both the filtered progress variable source term $\overline{\dot{\omega}}$ and the unresolved scalar transport terms τ_{D_c} and τ_c, respectively the transport of c by unresolved fluctuations of molecular diffusive flux and momentum,

$$\tau_D = \overline{\rho D_c(c)\nabla c} - \overline{\rho} D_c(\tilde{c})\nabla\tilde{c}\,, \quad (9)$$

$$\tau_c = \overline{\rho \mathbf{u} c} - \overline{\rho}\tilde{\mathbf{u}}\tilde{c}\,, \quad (10)$$

where $\mathbf{u}$ is the velocity vector. The networks are trained from image-type deep learning (convolutional) to build mapping functions, such that the filtered non-linear terms are expressed through the networks from their values computed from the resolved fields:

$$\overline{\dot{\omega}}(\underline{x},t) = \mathcal{G}\left[\dot{\omega}(\tilde{c}(\underline{x}_1,t)),\cdots,\dot{\omega}(\tilde{c}(\underline{x}_N,t))\right]\,, \quad (11)$$

where $\tilde{c}(\underline{x}_j,t)$ is known from LES, with $\underline{x}_j$ the N points selected around $\underline{x}$ to build the input image of the network (Fig. 8). The LES mesh size to resolve with $n = 5$ points the filtered progress variable can be estimated from

$$h = (\Delta/n)\sqrt{\pi/6 + \delta_L^2/\Delta^2}\,, \quad (12)$$

where Δ is the LES filter size [262]. On this basis, a three-dimensional test-box of size $(2h)^3$ is built from every of the M = 28.58 million DNS nodes. This 27-point $\underline{x}_j$ test box centered at $\underline{x}$ contains the three-dimensional distributions of $\dot{\omega}(\tilde{c}(\underline{x}_j,t))$ and $\nabla\cdot\left(\overline{\rho}D_c(\tilde{c})\nabla\tilde{c}\right)(\underline{x}_j,t)$. These data are stored as the 'images' that will be processed by the CNN as shown in Fig. 8. The 'labels' of each i-th image are $\overline{\dot{\omega}}[i] = \overline{\dot{\omega}}(\underline{x},t)$ and $\nabla\cdot\tau[i] = \nabla\cdot\left(\tau_D(\underline{x},t) - \tau_c(\underline{x},t)\right)$ for $i = 1,\cdots,N_L$. Two networks of similar structures (same number of layers, convolution kernels, etc.) are trained for the chemical source and for the SGS fluxes.

Results obtained for the filtered source terms are shown in Fig. 9. For the filter sizes seen by the neural networks during training ($\Delta = 0.3$ and 0.9 mm), the CNN predicts very well the filtered chemical source, with a good reproduction of the shape expected for this level of filtering/averaging [269], which is far from the Arrhenius-type response. Some departure from the DNS reference value is observed for the untrained case, but still much less than with 1D tabulated flame deconvolution discussed above, where the error could reach up to 25% for $\Delta = 3\delta_L$ [77]. With neural networks, the maximum error is of the order of 1% on the trained database and 16% for the untrained ones.

3.2. Flow resolved simulations of bluff-body flames

The next step is to extend DNS to the full domain covered by a laboratory turbulent flame. Figure 10 shows the 1.6 billion cells simulation [27] of the Cambridge University and Sandia National Laboratories turbulent lean premixed methane-air bluff-body burner [270, 271] (Resolution of 100 μm shown to be about twice the Kolmogorov scale, as expected in DNS [249], and sufficient to resolve the tabulated detailed chemistry, see Figs. 3, 4 and 6 in [27].) Statistical means can then be computed to validate DNS against measurements, for both velocity and scalars fields (Fig. 11), before probing the database for further analysis.

The testing of combustion models is performed both a-priori [27] and also a-posteriori, after coarsening the mesh for LES [65] of the same burner. These DNS databases are also useful to revisit turbulent combustion concepts, as for instance combustion regime diagrams [251]. Figure 12 shows that the combustion regime is not unique in this burner, but depends on both the position from the burner exit and the position within the mean turbulent flame brush. The diagrams for the unburned side of the flame suggest combustion in the thin reaction zone regime. However, the corrugated flamelets regime is observed for larger levels of progress of reaction. Some of the scatter plots are even multi-modal, in line with the competition between the different levels of turbulence of the two inlet streams and of the shear layers downstream of the bluff body. All these regimes actually interact to drive the dynamics of the turbulent flame.

The broad range of varying fluctuation levels observed in these DNS is clearly a plus for analysing the reacting flow physics, because flames in real com-

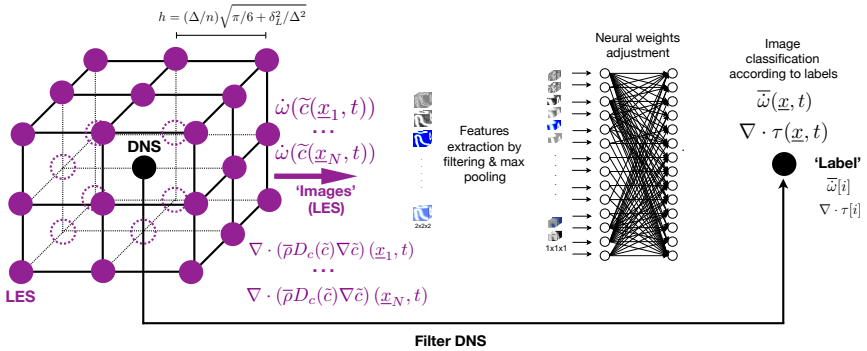

Fig. 8: CNN training from DNS, sketch of the database construction. Reprinted with permission [267].

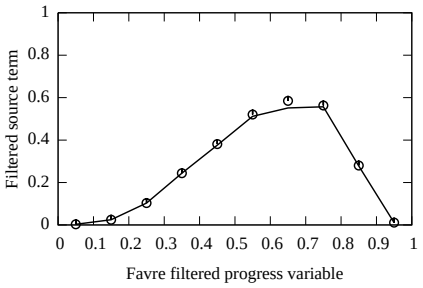

(a) Trained database. $\Delta = 0.30$ mm

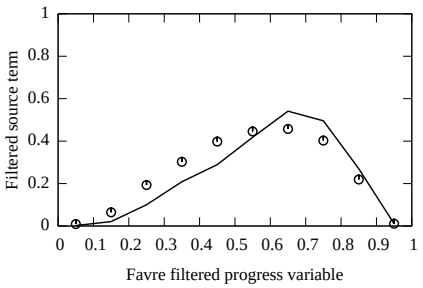

(b) Untrained database. $\Delta = 0.45$ mm

Fig. 9: $\left\langle \overline{\dot{\omega}^+} \mid \tilde{c} \right\rangle$ conditional mean of the normalised progress variable source vs $\tilde{c}$. Symbols: DNS reference. Line: CNN prediction. Reprinted with permission [267].

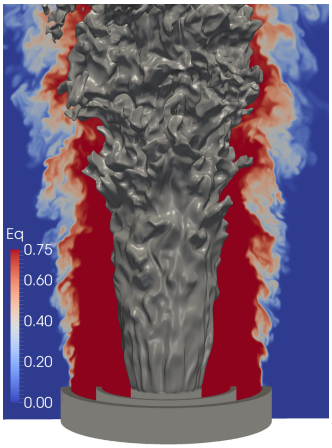

Fig. 10: Contour plot of equivalence ratio in a bluff-body burner mid-section, superimposed is an iso-surface for a progress variable value of $c = 0.5$. Reprinted with permission [27].

bustion systems feature a strong multi-scale character [272]. Chemistry was tabulated from freely propagating premixed flamelets. It would be valuable to perform the same DNS with detailed chemistry, to then evaluate the flamelet manifold hypothesis in situ (effect of curvature, unsteady strain, etc.).

4. Advancing numerics through machine learning and DNS

DNS provides unique opportunities to explore machine learning based approaches [139, 167, 173, 175, 264, 273–275] (and multiple references therein). In addition to neural network modeling already discussed above (Fig. 9), novel ideas to improve or speed-up the numerics can be tested, before implementing them in LES or RANS.

Figure 13 shows DNS of a syngas flame interacting with a cooled wall, which is at the origin of a strategy to reduce by more than an order of magnitude the CPU time devoted to integration of numerically stiff detailed chemistry. In this approach [215], artificial neural networks (ANN) are trained to return the increments of thermochemical quantities for a large set of input conditions. This is achieved aside from DNS or any flow simulation, using a turbulent non-adiabatic non-premixed micro-mixing based canonical problem coupled to a reference detailed chemistry. Heat-loss effects are included in the ANN training. Then, DNS is performed either with the ANN or with the direct solution of the stiff chemistry. The ANN chemistry provides a good agreement with Arrhenius-based detailed and reduced mechanisms (Fig. 14). It is 25 times faster in terms of CPU cost than the detailed

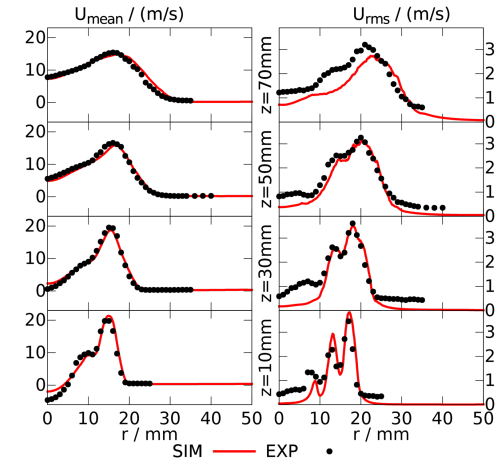

(a) Streamwise velocity

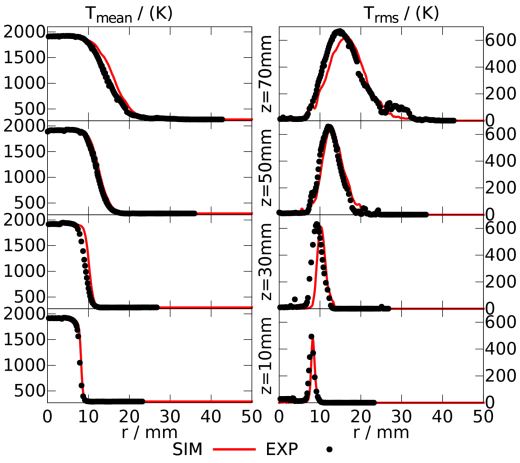

(b) Temperature

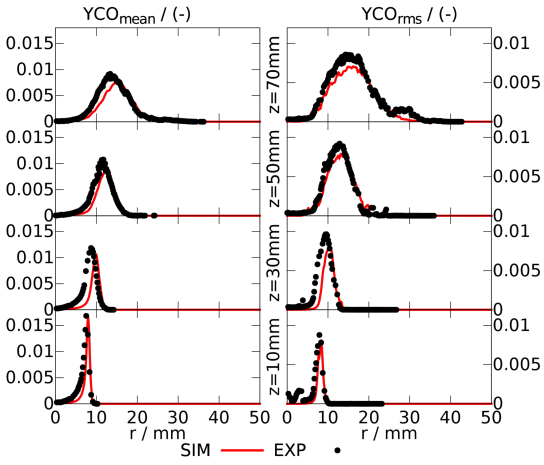

(c) CO mass fraction

Fig. 11: Comparison of statistical mean and RMS at different axial positions against experimental data [270, 271]. Reprinted with permission [27].

mechanism and 3 times faster than the reduced mechanism having the same number of species.

DNS is thus also very valuable to test novel numerical procedures. Basic tests can be conducted including the transport phenomena to which these numerical approaches will be coupled during the simulation of real combustion systems. With DNS, this can be done excluding the risk of multiple interferences between numerics and sub-grid scale models, which could potentially interact with the method under evaluation.

5. An alternative approach to canonical reactive flow DNS: Downsizing of real geometries

The usual approach to simulate three-dimensional flows in real combustion devices with a limited amount of grid cells, consists of artificially dissipating the smallest scales of the turbulence by increasing the flow viscosity. This is done in proportion to the turbulent Reynolds number, estimated either from the turbulence integral length scale (RANS) or from the cell size (LES). The nature of the fluid is then modified. An alternative approach based on DNS can be adopted [31, 276]. It consists of downsizing the system length, thus the global Reynolds number of the flow, instead of modifying the fluid properties. This second option can be valuable when the turbulence chemistry interaction at small scales dominates the progress of the chemical reactions and for turbulent flows with a large range of length and time scales. It corresponds to flows which feature a significant reservoir of large eddies, as typically large-scale boilers and furnaces. The simulation cost is mitigated by decreasing the residence time after reducing the system lengths, keeping unchanged the fluid properties, the bulk flow velocity and the kinetic turbulent energy.

Let us consider lengths scaled by a factor $\beta < 1$, then $\ell^\star = \beta\ell$, with ℓ the length of the real system and $\ell^\star$ its value in the DNS lab-scale model. The multicomponent flow properties (temperature, pressure, density, heat capacities, viscosity) are those of the real fluid. Mass flow rate ratios between inlets and velocities $u^\star = u$ are also those of the real system. Hence, the residence time τ_R is reduced by β, $\tau^\star = \beta\tau_R$. Doing so, the intensity of the turbulence fluctuations is left unchanged:

$$k^{\star\,1/2} \approx \ell_T^\star \left|\frac{\partial\widetilde{u^\star}}{\partial y^\star}\right| = \beta\ell_T \left|\frac{1}{\beta}\frac{\partial\widetilde{u}}{\partial y}\right| = k^{1/2}\,. \quad (13)$$

The turbulent Reynolds number is reduced by the factor β:

$$Re_T^\star = \frac{k^{1/2}\beta\ell_T}{\nu} = \beta Re_T\,, \quad (14)$$

the Kolmogorov scale is reduced by the factor $\beta^{1/4}$:

$$\eta_k^\star \approx \frac{\ell_T^\star}{Re_T^{\star\,3/4}} = \frac{\beta\ell_T}{(\beta Re_T)^{3/4}} = \beta^{1/4}\eta_k\,, \quad (15)$$

the dissipation rate is increase by β^{-1}:

$$\epsilon^\star \approx \frac{\nu^3}{\eta_k^{\star 4}} = \frac{\nu^3}{(\beta^{1/4}\eta_k)^4} = \frac{\epsilon}{\beta}\,. \quad (16)$$

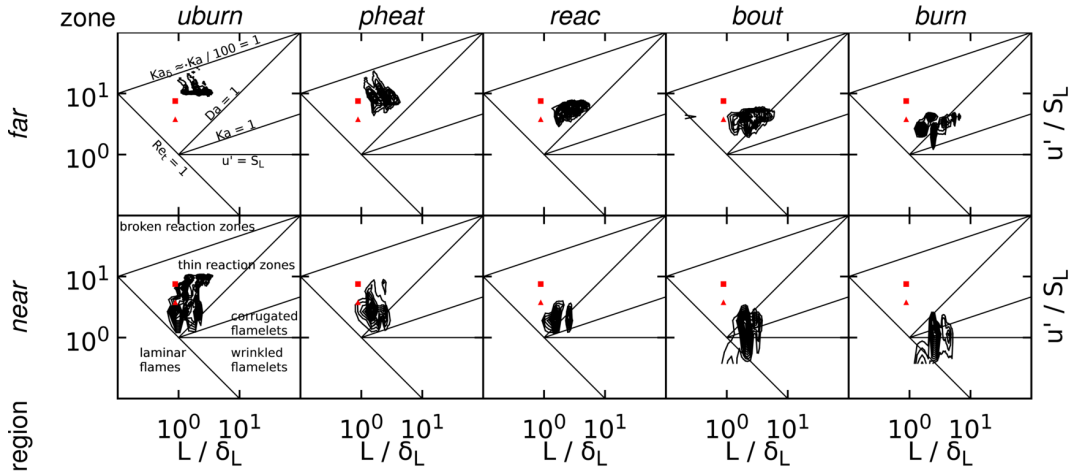

Fig. 12: Combustion regime diagrams with the conditioned joint PDFs of the velocity fluctuations normalized by the laminar flame speed vs the integral lengthscale of the velocity fluctuations normalized by the laminar flame thickness. Uburn: progress variable $c \in [0.01, 0.02]$; pheat: $c \in [0.6, 0.8]$; reac: max gradient of CH_3; bout: $c \in [0, 8, 0.98]$; burned $c \in [0.98, 0.99]$. The inlet conditions for the inner and outer stream are marked by triangles and squares, respectively. The different plots represent the conditioning on increasing height above the burner from bottom to top and increasing progress of the reaction from left to right. Reprinted with permission [27].

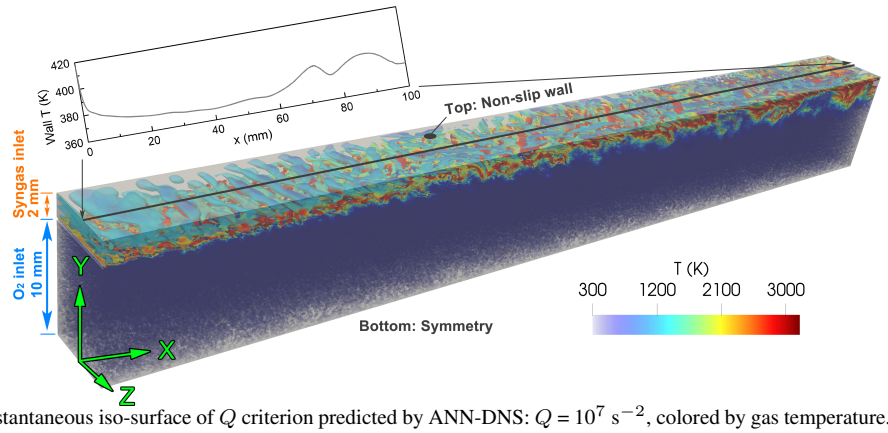

Fig. 13: Instantaneous iso-surface of Q criterion predicted by ANN-DNS: $Q = 10^7$ s^{-2}, colored by gas temperature. Top graph: distribution of instantaneous wall temperature along the centreline. Reprinted with permission [215].

The macro- and micro-mixing times become:

$$\tau_T^\star = \frac{k^\star}{\epsilon^\star} = \beta \frac{k}{\epsilon} = \beta \tau_T \,, \tag{17}$$

$$\tau_k^\star = \left(\frac{\nu}{\epsilon^\star}\right)^{1/2} = \left(\frac{\beta\nu}{\epsilon}\right)^{1/2} = \beta^{1/2}\tau_k \,. \tag{18}$$

To preserve the Damköhler number of the full-size system, the chemical time scales should be rescaled as[1]: $\tau_c^\star = \beta \tau_c$,

$$Da^\star = \frac{\tau_T^\star}{\tau_c^\star} = \frac{\beta\tau_T}{\beta\tau_c} = Da \,. \tag{19}$$

To preserve the Karlovitz number, a different scaling of the chemistry, $\tau_c^\star = \beta^{1/2}\tau_c$, must be used

$$Ka^\star = \frac{\tau_c^\star}{\tau_k^\star} = \frac{\tau_c^\star}{\beta^{1/2}\tau_k} = \frac{\beta^{1/2}\tau_c}{\beta^{1/2}\tau_k} = Ka \,. \tag{20}$$

From (19) and (20) a choice must be made between preserving Da or Ka. In practice, in real combustion chambers, the two scalings of the chemistry in β or $\beta^{1/2}$ may be related to two asymptotic flow regimes, which can be identified from a flow length scale and a scalar length scale:

$$\ell(\underline{x}, t) = \frac{[u(\underline{x}, t)|}{|\mathcal{S}(\underline{x}, t)|}, \quad \ell_\phi(\underline{x}, t) = \frac{\phi_{\max} - \phi_{\min}}{|\nabla\phi|\,(\underline{x}, t)} \,, \tag{21}$$

where $|\mathcal{S}(\underline{x}, t)|$ is the magnitude of the deformation tensor $\mathcal{S}_{ij} = 0.5[(\partial u_i/\partial x_j) + (\partial u_j/\partial x_i)]$.

[1] This is easily done by multiplying by β^{-1} all the pre-exponential factors of the chemical scheme.

When $\ell_\phi << \ell$, the scalar gradients occur over distances smaller than flow length scales, indicating a convective-like mode of the scalar field (*i.e.* as in a local plug flow), then a linear scaling of the chemical time is relevant. In the situations where $\ell_\phi >> \ell$, the small scale velocity fluctuations have entered the local scalar mixing layers, indicating a micro-mixing mode of the scalar field, then a square root scaling of the chemical time should be used. A dynamic rescaling of the chemical time scales that depend on the flow regime can then be established.

This approach was extended to carrier-phase liquid spray quasi-DNS, in order to preserve the statistical behavior of the liquid within the downsized version. After testing it in canonical DNS configurations, it was applied to an incinerator including a selective urea-based non-catalytic slow chemistry NOx reduction (SNCR DeNOx) [31]. This incinerator of about 10 MW is a cylinder of 16.0 m long with a diameter of 4.45 m. Liquid and gaseous flows are injected at the four axial locations 'A', 'B', 'C' and 'D' in Fig. 15, providing a total mass flow rate $\dot{Q}_m$ in the system. The bottom stage carries cooling air (stage A) through a six-inlet crown, for a contribution of $0.1\dot{Q}_m$. Burnt gases produced by burners are injected at stage B through three large inlets ($0.54\dot{Q}_m$), the flow temperatures in these three inlets are 1990 K, 1840 K and 2300 K, respectively. Three additional pipes inject additional cooling air at this stage B ($0.05\dot{Q}_m$). The water sprays carrying the chemical waste are injected with air at stage C, through a four-inlet crown, contributing to $0.2\dot{Q}_m$. At stage D, two more injection pipes bring $0.11\dot{Q}_m$ of water spray polluted with the nitrogenous chemical waste, the other inlet at stage D is carrying liquid water with urea for NO reduction (the third pipe at this position is not in use).

Imposing a downsizing factor $\beta = 1/30$, a simulation resolving the Kolmogorov scale with a mesh spacing $h = 150\mu$m in the shear layers for 162 million cells has been conducted with a fourth-order unstructured flow solver [277]. A reduced chemical scheme describes the reactions at play [278]. This simulation was first validated against statistics from in-situ measurements and LES (details about chemistry, numerics and the validation procedure may be found in [31]).

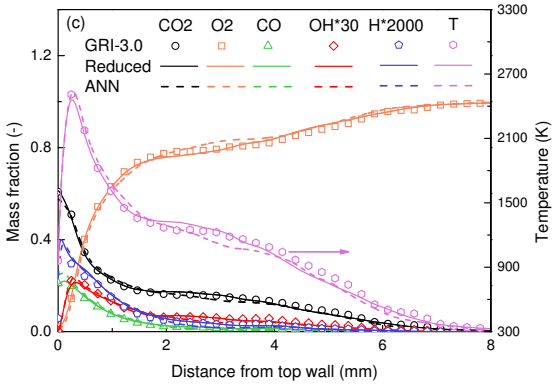

Fig. 14: Spanwise averaged distributions of CO_2, O_2, CO, OH, H mass fractions and temperature. Symbols: detailed chemistry GRI-3.0 [256] Solid line: Reduced mechanism (Table 2 in [215]). Dashed line with symbols: ANN chemistry. 80 mm from the nozzle inlet. Reprinted with permission [215].

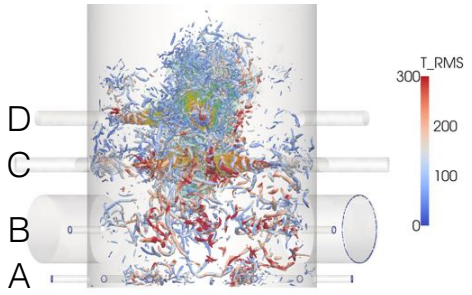

(a) Q-criterion colored by RMS temperature.

Fig. 15: Flow visualisation from unsteady simulations of SNCR in an incinerator. Reprinted with permission [31].

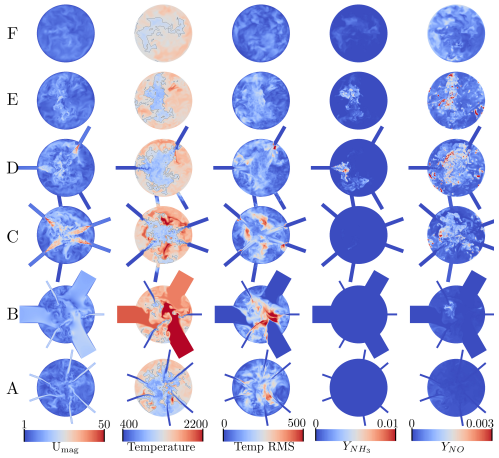

Fig. 16: Snapshots of instantaneous flow quantities with resolution $h = 150$ µm. From bottom to top, locations of Figure 15. Axial position $z_E = z_D + 1$ m, $z_F = z_D + 3$ m. Velocity magnitude in $\mathrm{m \cdot s^{-1}}$. Temperature in K, black line: iso-temperature at 1200 K. Reprinted with permission [31].

Such flow and chemistry resolved simulation provides unique and very detailed information on the mixing and reactions inside the incinerator (Fig. 16), specifically concerning the NOx evolutions. Subtle modifications of the geometry of the injection systems can be envisioned and tested. For instance, it is seen in Fig. 16 that the temperature is not homoge-

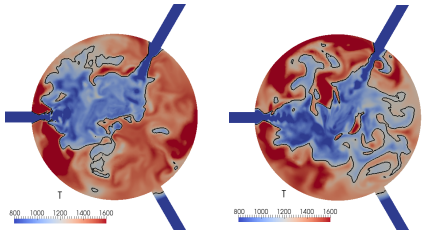

(a) Original design (b) Improved design

Fig. 17: Impact of improved injection design on temperature levels favouring DeNOx.

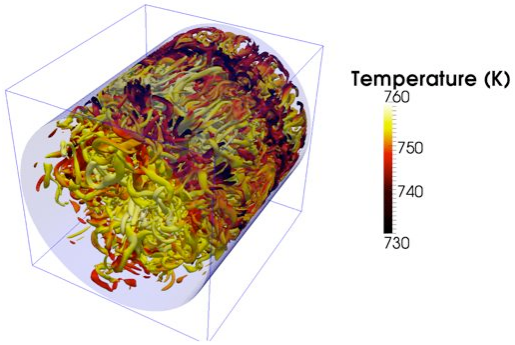

Fig. 18: Iso-contour of Q-criterion ($Q = 15 \cdot 10^6$ s^{-2}) colored by temperature in DNS of a rapid compression machine. Flow goes from left to right. Reprinted with permission [276].

neous traveling downstream, with levels well above 1200 K, for an optimal DeNOx process operating between 1150 K and 1250 K. The results suggest to modify the injection of cooling water at stage C, so that a weakly evolving swirling motion develops inside the furnace. The impact on the temperature distribution in the plane D of such modification is seen in Fig. 17. The flow zone where the temperature is below 1200 K is enlarged after modifying the injection, with an efficiency of the DeNOx process improved by 7%, which was also observed in the real system after implementing the novel injection.

This level of information could not be obtained from unsteady simulations of the whole system in its full size. Indeed, for the same number of grids nodes, LES of the full system leads to a resolution of 5 mm, which was not found enough to capture the detail of the turbulence mixing processes driving the DeNOx.

The quasi-DNS of lab-scale version of furnaces may thus be of great interest to understand the role of geometrical details and envision roadmaps to improve their performance. Lab-scale DNS was also applied to a rapid compression machine after downsizing its geometry [276, 279], to quantify the impact of heat transfer at wall and the effect of weak pressure waves on undesirable ignitions (Fig. 18).

6. DNS Carbon footprint

With actual global warming concerns and because the ultimate objective of DNS is to help improving combustion systems efficiency, and before concluding, it seems relevant to discuss the CO_2 footprint of these simulations and, eventually, of the storage of databases.

The estimation of this footprint is influenced by numerous parameters: the amount of processors CPU time which were necessary, in direct relation with the mesh size and the complexity of the thermochemical model introduced [280], the overhead of the computing facilities and how electricity was produced (i.e., the geographic location of the computing center).

Considering a DNS featuring 2 billion degrees of freedom (number of mesh cells) running for one week on 10 000 cores with a low-Mach solver and using tabulated chemistry in the lean premixed regime, about 1.68 million hours are needed. Run in France on Xeon Platinum 9282, which is a power efficient processor (base frequency 2,6GHz, 77 MB Intel Smart Cache), according to [281, 282], this DNS cost 776 kg of CO_2 equivalent (CO_2e). This amount corresponds to 6000 km in a passenger car (130 g CO_2/km) or to 70 years of carbon sequestration by a tree. For a computing center in Vancouver, the cost is much lower, only 255 kg of CO_2e, thanks to its electricity production based on hydropower. With electricity produced from coal, the cost rises dramatically up to 11 000 kg of CO_2e (1000 years of carbon sequestration by a tree).

A more global approach may be followed, which also includes the manufacturing of the computer, the storage during the computation, the interconnecting network and the manpower necessary to manage the computing center [283]. Then, to compensate for the 1.68 million hours DNS on the GRICAD computing center located in Grenoble, France, up 500 years of carbon sequestration by a tree would be necessary.

If we were to compensate for our simulations by planting trees, the planet would rapidly be green again! It must be acknowledged that this issue is generally present in all applications of high-performance computing, from fluid mechanics (reactive or non-reactive flows) to quantum chromodynamics (QCD).

We should try our best to alleviate these CO_2 cost of DNS by a global effort to rationalise the use of the databases and the promotion of their sharing.

7. Summary and perspectives

Over the past few years, direct numerical simulation of turbulent flames has evolved from a tool devoted to theoretical combustion, towards one of the standard ingredients of numerical combustion bringing information useful for progressing in the optimisation and the design of combustion systems.

Initially limited to canonical flows featuring peri-

odic boundary conditions (homogeneous turbulence, mixing layers), DNS can now be applied to laboratory jet flames (premixed and nonpremixed), opening many perspectives: firstly, because one can now validate DNS results against experiments, and secondly, because the reacting flow physics subtleties controling those turbulent flames is more likely to ressemble to those of real burners.

Because flames in many combustion chambers are actually developing over less than one meter long and away from walls, challenges in combustion DNS differ from those faced by external flows aerodynamics, where very high Reynolds number boundary layers developing over many meters are present. Accordingly, thanks to the continuous development of computing efficiency combining progress in code architecture and the availability of petaflops-class computers, the gap is progressively closing between DNS and high fidelity LES. The boundary between these two numerical descriptions of reactive flows getting progressively blurred. This trend needs to be accompanied by a reflection in the DNS community, to keep the correct balance between securing numerical accuracy and addressing configurations useful for improving combustion systems.

DNS generates huge databases feeding the flourishing machine learning techniques and the number of studies in this field is exponentially growing. Physics-informed techniques [284], in which the iterative solution of PDE is fully coupled with the training of neural networks, will certainly soon open new perspectives in combustion DNS.

References

[1] S. A. Orszag, Analytical theories of turbulence, J. Fluid Mech. 41 (2) (1970) 363–386.

[2] J. R. Herring, R. M. Kerr, Comparison of direct numerical simulations with predictions of two-point closures for isotropic turbulence convecting a passive scalar, J. Fluid Mech. 118 (1982) 205–219.

[3] V. Eswaran, S. B. Pope, Direct numerical simulation of the turbulent mixing of a passive scalar, Phys. Fluids 31 (3) (1988) 506–520.

[4] R. S. Rogallo, P. Moin, Numerical simulation of turbulent flows, Annual Review Fluid Mech. 16 (1984) 99–137.

[5] A. D. Leonard, J. C. Hill, Direct simulation of turbulent flows with chemical reaction, J. Sci. Comput. 3 (1988) 25–43.

[6] C. Rutland, S. E. Tahry, J. H. Ferziger, Direct simulation of turbulent pre-mixed reacting flows, Am. Phys. Soc. 32 (1987) 2032.

[7] C. J. Montgomery, G. Kosaly, J. J. Riley, Direct numerical simulation of turbulent reacting flow using a reduced hydrogen-oxygen mechanism, Combust. Flame 95 (3) (1993) 247–260.

[8] T. Poinsot, D. Veynante, S. Candel, Quenching processes and premixed turbulent combustion diagrams, J. Fluid Mech. 228 (1991) 561–606.

[9] P. Domingo, L. Vervisch, Triple flames and partially premixed combustion in autoignition of non-premixed mixtures, in: Symp. (Int.) on Combust., Vol. 26, 1996, pp. 233–240.

[10] L. Vervisch, T. Poinsot, Direct numerical simulation of non-premixed turbulent flames, Annual Review Fluid Mech. 30 (1998) 655–691.

[11] M. Baum, T. Poinsot, D. Haworth, D. Darabiha, Direct numerical simulation of $H_2/O_2/N_2$ flames with complex chemistry in two-dimensional turbulent flows, J. Fluid Mech. 281 (1994) 1–32.

[12] F. Mashayek, Numerical investigation of reacting droplets in homogeneous shear turbulence, J. Fluid Mech. 405 (2000) 1–36.

[13] J. Réveillon, L. Vervisch, Spray vaporization in non-premixed turbulent flames: a single droplet model, Combust. Flame 121 (1/2) (2000) 75–90.

[14] J. Reveillon, L. Vervisch, Analysis of weakly turbulent diluted-spray flames and combustion regimes, J. Fluid Mech. (2005) 317–347.

[15] A. Shamooni, P. Debiagi, B. Wang, T. D. Luu, O. T. Stein, A. Kronenburg, G. Bagheri, A. Stagni, A. Frassoldati, T. Faravelli, A. M. Kempf, X. Wen, C. Hasse, Carrier-phase DNS of detailed NOx formation in early-stage pulverized coal combustion with fuel-bound nitrogen, Fuel 291 (2021) 119998.

[16] A. Nonaka, M. S. Day, J. B. Bell, A conservative, thermodynamically consistent numerical approach for low mach number combustion. Part I: Single-level integration, Combust. Theory Modelling 22 (1) (2018) 156–184.

[17] V. Giovangigli, Multicomponent Flow Modeling, Modeling and Simulation in Science, Engineering and Technology, Birkhäuser, Springer, 1999.

[18] J. H. Chen, Petascale direct numerical simulation of turbulent combustion—fundamental insights towards predictive models, Proc. Comb. Inst. 33 (1) (2011) 99–123.

[19] M. Emmett, E. Motheau, W. Zhang, M. Minion, J. B. Bell, A fourth-order adaptive mesh refinement algorithm for the multicomponent, reacting compressible Navier-Stokes equations, Combust. Theory Modelling 23 (4) (2019) 592–625.

[20] J. Bell, M. Day, Adaptive Methods for Simulation of Turbulent Combustion, Springer Netherlands, 2011, Ch. 13, pp. 301–329.

[21] H. Wang, E. R. Hawkes, J. H. Chen, A direct numerical simulation study of flame structure and stabilization of an experimental high Ka CH4/air premixed jet flame, Combust. Flame 180 (2017) 110–123.

[22] D. Gottlieb, S. A. Orszag, Numerical Analysis of Spectral Methods: Theory and Applications, SIAM, 1977.

[23] S. K. Lele, Compact finite difference schemes with spectral like resolution, J. Comput. Phys. 103 (1992) 16–42.

[24] T. Poinsot, S. K. Lele, Boundary conditions for direct simulations of compressible viscous flows, J. Comput. Phys. 1 (101) (1992) 104–129.

[25] D. T. M. Baum, T. Poinsot, Accurate boundary conditions for multicomponent reactive flow, J. Comput. Phys. 116 (1994) 247–261.

[26] G. Lodato, P. Domingo, L. Vervisch, Three-dimensional boundary conditions for Direct and Large-Eddy Simulation of compressible viscous flows, J. Comput. Phys 227 (10) (2008) 5105–5143.

[27] F. Proch, P. Domingo, L. Vervisch, A. Kempf, Flame resolved simulation of a turbulent premixed bluff-body burner experiment. Part i: Analysis of the reaction zone dynamics with tabulated chemistry, Combust. Flame 180 (2017) 321–339.

[28] T. Zirwes, F. Zhang, P. Habisreuther, M. Hansinger, H. Bockhorn, M. Pfitzner, D. Trimis, Quasi-DNS dataset of a piloted flame with inhomogeneous inlet conditions, Flow Turbulence Combust. 104 (4) (2020) 997–1027.

[29] S. Enger, B. Basu, M. Breuer, F. Durst, Numerical study of three-dimensional mixed convection due to buoyancy and centrifugal force in an oxide melt for czochralski growth, J. Cryst. Growth 219 (2000) 144–164.

[30] E. Kome, L. Camilo, A. Shams, B. J. Geurts, B. Koren, A quantification method for numerical dissipation in quasi-dns and under-resolved dns, and effects of numerical dissipation in quasi-dns and under-resolved dns of turbulent channel flows, J. Comput. Phys. 345 (2017) 565–595.

[31] B. Farcy, L. Vervisch, P. Domingo, Large Eddy Simulation of selective non-catalytic reduction (SNCR): A downsizing procedure for simulating nitric-oxide reduction units, Chem. Eng. Sci. 139 (2016) 285–303.

[32] W. Han, A. Scholtissek, F. Dietzsch, C. Hasse, Thermal and chemical effects of differential diffusion in turbulent non-premixed H-2 flames, Proc. Combust. Inst. 38 (2) (2021) 2627–2634.

[33] C. T. d'Auzay, V. Papapostolou, N. Chakraborty, Effects of biogas composition on the edge flame propagation in ignition turbulent mixing layers, Flow turbulence Combust. 106 (2021) 1437–1459.

[34] A. Jameson, A proof of the stability of the spectral difference method for all orders of accuracy, J. Sci. Comput. 45 (1) (2010) 348–358.

[35] G. K. Giannakopoulos, C. E. Frouzakis, P. F. Fischer, A. G. Tomboulides, K. Boulouchos, LES of the gas-exchange process inside an internal combustion engine using a high-order method, Flow Turbulence Combust. 104 (2) (2020) 673–692.

[36] N. Tonicellò, G. Lodato, L. Vervisch, Turbulence kinetic energy transfers in direct numerical simulation of shock-wave-turbulence interaction in a compression/expansion ramp, J. Fluid Mech. 935:A31 (A31) (2022) 1–43.

[37] S. Lapointe, G. Blanquart, A priori filtered chemical source term modeling for LES of high Karlovitz number premixed flames, Combust. Flame 176 (2017) 500–510.

[38] A. J. Fillo, J. Schlup, G. Blanquart, K. E. Niemeyer, Assessing the impact of multicomponent diffusion in direct numerical simulations of premixed, high-Karlovitz, turbulent flames, Combust. Flame 223 (2021) 216–229.

[39] L. Cifuentes, C. Dopazo, J. Martin, P. Domingo, L. Vervisch, Effects of the local flow topologies upon the structure of a premixed methane-air turbulent jet flame, Flow Turbulence Combust. 96 (2) (2016) 535–546.

[40] D. Veynante, A. Trouvé, K. Bray, T. Mantel, Gradient and counter-gradient scalar transport in turbulent premixed flames, J. Fluid Mech. 332 (1997) 263–293.

[41] H. Wang, E. R. Hawkes, J. H. Chen, B. Zhou, Z. Li, M. Alden, Direct numerical simulations of a high Karlovitz number laboratory premixed jet flame - An analysis of flame stretch and flame thickening, J. Fluid Mech. 815 (2017) 511–536.

[42] T. Nilsson, H. Carlsson, R. Yu, X.-S. Bai, Structures of turbulent premixed flames in the high karlovitz number regime - DNS analysis, Fuel 216 (2018) 627–638.

[43] J. F. MacArt, T. Grenga, M. E. Mueller, Effects of combustion heat release on velocity and scalar statistics in turbulent premixed jet flames at low and high Karlovitz numbers, Combust. Flame 191 (2018) 468–485.

[44] V. Raman, M. Hassanaly, Emerging trends in numerical simulations of combustion systems, Proc. Comb. Inst. 37 (2) (2019) 2073–2089.

[45] J. F. Driscoll, J. H. Chen, A. W. Skiba, C. D. Carter, E. R. Hawkes, H. Wang, Premixed flames subjected to extreme turbulence: Some questions and recent answers, Prog. Energy Combust. Sci. 76 (2020) 100802.

[46] A. N. Lipatnikov, Stratified turbulent flames: Recent advances in understanding the influence of mixture inhomogeneities on premixed combustion and modeling challenges, Prog. Energy Combust. Sci. 62 (2017) 87–132.

[47] H. Im, Modeling and Simulation of Turbulent Combustion. Energy, Environment, and Sustainability, De S., Agarwal A., Chaudhuri S., Sen S. Edition, Springer, Singapore, 2018, Ch. Direct Numerical Simulations for Combustion Science: Past, Present, and Future, pp. 99–134.

[48] P. Trisjono, H. Pitsch, Systematic analysis strategies for the development of combustion models from DNS: A review, Flow Turbulence Combust. 95 (2015) 231–259.

[49] P. E. Hamlington, A. Y. Poludnenko, E. S. Oran, Interactions between turbulence and flames in premixed reacting flows, Phys. Fluids 23 (2011) 125111.

[50] H. Wang, E. R. Hawkes, B. Zhou, J. H. Chen, Z. Li, M. Alden, A comparison between direct numerical simulation and experiment of the turbulent burning velocity-related statistics in a turbulent methane-air premixed jet flame at high Karlovitz number, Proc. Combust. Institute 36 (2) (2017) 2045–2053.

[51] C. J. Lapeyre, A. Misdariis, N. Cazard, D. Veynante, T. Poinsot, Training convolutional neural networks to estimate turbulent sub-grid scale reaction rates, Combust. Flame 203 (2019) 255–264.

[52] F. Qin, A. Shah, Z.-w. Huang, L.-n. Peng, P. Tunestal, X.-S. Bai, Detailed numerical simulation of transient mixing and combustion of premixed methane/air mixtures in a pre-chamber/main-chamber system relevant to internal combustion engines, Combust. Flame 188 (2018) 357–366.

[53] C. Xu, J.-W. Park, C. S. Yoo, J. H. Chen, T. Lu, Identification of premixed flame propagation modes using chemical explosive mode analysis, Proc. Combust. Inst. 37 (2) (2019) 2407–2415.

[54] G. Nivarti, S. Cant, Direct Numerical Simulation of the bending effect in turbulent premixed flames, Proc. Combust. Inst. 36 (2) (2017) 1903–1910.

[55] M. Klein, N. Chakraborty, S. Ketterl, A comparison of strategies for direct numerical simulation of turbulence chemistry interaction in generic planar turbulent premixed flames, Flow Turbulence Combust. 99 (3-4) (2017) 955–971.

[56] S. Luca, A. Attili, E. Lo Schiavo, F. Creta, F. Bisetti, On the statistics of flame stretch in turbulent premixed jet flames in the thin reaction zone regime at varying Reynolds number, Proc. Combust. Inst. 37 (2) (2019) 2451–2459.

[57] G. Ribert, P. Domingo, L. Vervisch, Analysis of subgrid scale modeling of the ideal-gas equation of state in hydrogen-oxygen premixed flames, Proc. Combust. Inst. 37 (2019) 2345–2351.

[58] C. Jainski, M. Rissmann, B. Boehm, A. Dreizler, Experimental investigation of flame surface density and mean reaction rate during flame-wall interaction, Proc. Combust. Inst. 36 (2) (2017) 1827–1834.

[59] V. A. Sabelnikov, A. N. Lipatnikov, N. Chakraborty, S. Nishiki, T. Hasegawa, A balance equation for the mean rate of product creation in premixed turbulent flames, Proc. Combust. Inst. 36 (2) (2017) 1893–1901.

[60] D. Dasgupta, W. Sun, M. Day, T. Lieuwen, Effect of turbulence-chemistry interactions on chemical pathways for turbulent hydrogen-air premixed flames, Combust. Flame 176 (2017) 191–201.

[61] R. Yu, A. N. Lipatnikov, DNS study of dependence of bulk consumption velocity in a constant-density reacting flow on turbulence and mixture characteristics, Phys. Fluids 29 (6) (2017).

[62] N. Chakraborty, D. Alwazzan, M. Klein, R. S. Cant, On the validity of Damkohler's first hypothesis in turbulent bunsen burner flames: A computational analysis, Proc. Combust. Inst 37 (2) (2019) 2231–2239.

[63] S. Zhong, F. Zhang, Z. Peng, F. Bai, Q. Du, Roles of CO2 and H2O in premixed turbulent oxy-fuel combustion, Fuel 234 (2018) 1044–1054.

[64] J. Sellmann, J. Lai, A. M. Kempf, N. Chakraborty, Flame surface density based modelling of head-on quenching of turbulent premixed flames, Proc. Combust. Inst. 36 (2) (2017).

[65] F. Proch, P. Domingo, L. Vervisch, A. M. Kempf, Flame resolved simulation of a turbulent premixed bluff-body burner experiment. Part ii: A-priori and a-posteriori investigation of sub-grid scale wrinkling closures in the context of artificially thickened flame modeling, Combust. Flame 180 (2017) 340–350.

[66] S. Yang, R. Ranjan, V. Yang, S. Menon, W. Sun, Parallel on-the-fly adaptive kinetics in direct numerical simulation of turbulent premixed flame, Proc. Combust. Inst. 36 (2) (2017) 2025–2032.

[67] W. Han, H. Wang, G. Kuenne, E. R. Hawkes, J. H. Chen, J. Janicka, C. Hasse, Large eddy simulation/dynamic thickened flame modeling of a high Karlovitz number turbulent premixed jet flame, Proc. Combust. Inst. 37 (2) (2019) 2555–2563.

[68] M. Klein, D. Alwazzan, N. Chakraborty, A direct numerical simulation analysis of pressure variation in turbulent premixed Bunsen burner flames-Part 1: Scalar gradient and strain rate statistics, Comput. Fluids 173 (2018) 178–188.

[69] M. Klein, C. Kasten, N. Chakraborty, N. Mukhadiyev, H. G. Im, Turbulent scalar fluxes in H-2-air premixed flames at low and high Karlovitz numbers, Combust. Theory Modelling 22 (6) (2018) 1033–1048.

[70] H. L. Dave, A. Mohan, S. Chaudhuri, Genesis and evolution of premixed flames in turbulence, Combust. Flame 196 (2018) 386–399.

[71] A. N. Lipatnikov, J. Chomiak, V. A. Sabelnikov, S. Nishiki, T. Hasegawa, A DNS study of the physical mechanisms associated with density ratio influence on turbulent burning velocity in premixed flames, Combust. Theory Modelling 22 (1) (2018) 131–155.

[72] N. A. K. Doan, N. Swaminathan, N. Chakraborty, Multiscale analysis of turbulence-flame interaction in premixed flames, Proc. Combust. Inst. 36 (2) (2017) 1929–1935.

[73] S. H. Kim, Leading points and heat release effects in turbulent premixed flames, Proc. Combust. Inst. 36 (2) (2017) 2017–2024.

[74] C. Turquand d'Auzay, V. Papapostolou, S. F. Ahmed, N. Chakraborty, On the minimum ignition energy and its transition in the localised forced ignition of turbulent homogeneous mixtures, Combust. Flame 201 (2019) 104–117.

[75] P. Zhao, L. Wang, N. Chakraborty, Analysis of the flame-wall interaction in premixed turbulent combustion, J. Fluid Mech. 848 (2018) 193–218.

[76] A. Haghiri, M. Talei, M. J. Brear, E. R. Hawkes, Sound generation by turbulent premixed flames, J. Fluid Mech. 843 (2018) 29–52.

[77] P. Domingo, L. Vervisch, DNS and approximate deconvolution as a tool to analyse one-dimensional filtered flame sub-grid scale modelling, Combust. Flame 177 (2017) 109–122.

[78] M. Kuron, Z. Ren, E. R. Hawkes, H. Zhou, H. Kolla, J. H. Chen, T. Lu, A mixing timescale model for TPDF simulations of turbulent premixed flames, Combust. Flame 177 (2017) 171–183.

[79] M. Klein, A. Herbert, H. Kosaka, B. Boehm, A. Dreizler, N. Chakraborty, V. Papapostolou, H. G. Im, J. Hasslberger, Evaluation of flame area based on detailed chemistry DNS of premixed turbulent hydrogen-air flames in different regimes of combustion, Flow Turbulence Combust. 104 (2-3) (2020) 403–419.

[80] A. N. Lipatnikov, V. A. Sabelnikov, S. Nishiki, T. Hasegawa, Letter: Does flame-generated vorticity increase turbulent burning velocity?, Phys. Fluids 30 (8) (2018).

[81] A. Validi, F. Jaberi, Numerical study of turbulent jet ignition in a lean premixed configuration, Flow Turbulence Combust. 100 (1) (2018) 197–224.

[82] V. A. Sabelnikov, R. Yu, A. N. Lipatnikov, Thin reaction zones in constant-density turbulent flows at low Damkohler numbers: Theory and simulations, Phys. Fluids 31 (5) (2019).

[83] A. N. Lipatnikov, V. A. Sabelnikov, S. Nishiki, T. Hasegawa, Combustion-induced local shear layers within premixed flamelets in weakly turbulent flows, Phys. Fluids 30 (8) (2018).

[84] T. M. Wabel, P. Zhang, X. Zhao, H. Wang, E. Hawkes, A. M. Steinberg, Assessment of chemical scalars for heat release rate measurement in highly turbulent premixed combustion including experimental factors, Combust. Flame 194 (2018) 485–506.

[85] V. A. Sabelnikov, A. N. Lipatnikov, S. Nishiki, T. Hasegawa, Investigation of the influence of combustion-induced thermal expansion on two-point turbulence statistics using conditioned structure functions, J. Fluid Mech. 867 (2019) 45–76.

[86] V. A. Sabelnikov, A. N. Lipatnikov, S. Nishiki, T. Hasegawa, Application of conditioned structure functions to exploring influence of premixed combustion on two-point turbulence statistics, Proc. Combust. Inst. 37 (2) (2019) 2433–2441.

[87] A. N. Lipatnikov, V. A. Sabelnikov, N. Chakraborty, S. Nishiki, T. Hasegawa, A DNS study of closure relations for convection flux term in transport equation for mean reaction rate in turbulent flow, Flow Turbulence Combust. 100 (1) (2018) 75–92.

[88] B. Savard, S. Lapointe, A. Teodorczyk, Numerical investigation of the effect of pressure on heat release rate in iso-octane premixed turbulent flames under conditions relevant to SI engines, Proc. Combust. Inst. 36 (3) (2017) 3543–3549.

[89] P. Trisjono, H. Pitsch, A direct numerical simulation study on NO formation in lean premixed flames, Proc. Combust. Inst. 36 (2) (2017) 2033–2043.
[90] D. Cecere, E. Giacomazzi, N. M. Arcidiacono, F. R. Picchia, Direct numerical simulation of high pressure turbulent lean premixed CH4/H-2 - Air slot flames, Int. J. Hydrogen Energy 43 (10) (2018) 5184–5198.
[91] J. Lai, A. Moody, N. Chakraborty, Turbulent kinetic energy transport in head-on quenching of turbulent premixed flames in the context of Reynolds Averaged Navier-Stokes simulations, Fuel 199 (2017) 456–477.
[92] D. M. Manias, E.-A. Tingas, Y. Minamoto, H. G. Im, Topological and chemical characteristics of turbulent flames at MILD conditions, Combust. Flame 208 (2019) 86–98.
[93] R. Yu, T. Nillson, X.-S. Bai, A. N. Lipatnikov, Evolution of averaged local premixed flame thickness in a turbulent flow, Combust. Flame 207 (2019) 232–249.
[94] M. Schoepplein, J. Weatheritt, R. Sandberg, M. Talei, M. Klein, Application of an evolutionary algorithm to LES modelling of turbulent transport in premixed flames, J. Comput. Phys. 374 (2018) 1166–1179.
[95] Y. Minamoto, B. Yenerdag, M. Tanahashi, Morphology and structure of hydrogen-air turbulent premixed flames, Combust. Flame 192 (2018) 369–383.
[96] Z. Wang, E. Motheau, J. Abraham, Effects of equivalence ratio variations on turbulent flame speed in lean methane/air mixtures under lean-burn natural gas engine operating conditions, Proc. Combust. Inst. 36 (2017) 3423–3430.
[97] S. Wiseman, M. Rieth, A. Gruber, J. R. Dawson, J. H. Chen, A comparison of the blow-out behavior of turbulent premixed ammonia/hydrogen/nitrogen-air and methane-air flames, Proc. Combust. Inst. 38 (2) (2021) 2869–2876.
[98] F. Creta, P. E. Lapenna, R. Lamioni, N. Fogla, M. Matalon, Propagation of premixed flames in the presence of Darrieus-Landau and thermal diffusive instabilities, Combust. Flame 216 (2020) 256–270.
[99] A. N. Lipatnikov, N. Chakraborty, V. A. Sabelnikov, Transport equations for reaction rate in laminar and turbulent premixed flames characterized by non-unity lewis number, Int. J. Hydrogen Energy 43 (45) (2018) 21060–21069.
[100] B. Savard, H. Wang, A. Teodorczyk, E. R. Hawkes, Low-temperature chemistry in n-heptane/air premixed turbulent flames, Combust. Flame 196 (2018) 71–84.
[101] M. Klein, D. Alwazzan, N. Chakraborty, A Direct Numerical Simulation analysis of pressure variation in turbulent premixed bunsen burner flames-part 2: Surface Density Function transport statistics, Comput. Fluids 173 (2018) 147–156.
[102] B. Savard, E. R. Hawkes, K. Aditya, H. Wang, J. H. Chen, Regimes of premixed turbulent spontaneous ignition and deflagration under gas-turbine reheat combustion conditions, Combust. Flame 208 (2019) 402–419.
[103] T. Nilsson, R. Yu, N. A. K. Doan, I. Langella, N. Swaminathan, X.-S. Bai, Filtered reaction rate modelling in moderate and high Karlovitz number flames: An a priori analysis, Flow Turbulence Combust. 103 (3) (2019) 643–665.
[104] J. F. MacArt, T. Grenga, M. E. Mueller, Evolution of flame-conditioned velocity statistics in turbulent premixed jet flames at low and high Karlovitz numbers, Proc. Combust. Inst. 37 (2) (2019) 2503–2510.
[105] S. Trivedi, R. Griffiths, H. Kolla, J. H. Chen, R. S. Cant, Topology of pocket formation in turbulent premixed flames, Proc. Combust. Inst. 37 (2) (2019) 2619–2626.
[106] X. Wang, T. Jin, Y. Xie, K. H. Luo, Pressure effects on flame structures and chemical pathways for lean premixed turbulent H-2/air flames: Three-dimensional DNS studies, Fuel 215 (2018) 320–329.
[107] P. Xavier, A. Ghani, D. Mejia, M. Miguel-Brebion, M. Bauerheim, L. Selle, T. Poinsot, Experimental and numerical investigation of flames stabilised behind rotating cylinders: interaction of flames with a moving wall, J. Fluid Mech. 813 (2017) 127–151.
[108] A. G. Novoselov, C. K. Law, M. E. Mueller, Direct Numerical Simulation of turbulent nonpremixed "cool" flames: Applicability of flamelet models, Proc. Combust. Inst. 37 (2) (2019) 2143–2150.
[109] C. Chi, A. Abdelsamie, D. Thevenin, Direct Numerical Simulations of hotspot-induced ignition in homogeneous hydrogen-air pre-mixtures and ignition spot tracking, Flow Turbulence Combust. 101 (1) (2018) 103–121.
[110] O. Owoyele, T. Echekki, Toward computationally efficient combustion DNS with complex fuels via principal component transport, Combust. Theory Modelling 21 (4) (2017) 770–798.
[111] D. Brouzet, A. Haghiri, M. Talei, M. J. Brear, Annihilation events topology and their generated sound in turbulent premixed flames, Combust. Flame 204 (2019) 268–277.
[112] A. N. Lipatnikov, S. Nishiki, T. Hasegawa, A DNS assessment of linear relations between filtered reaction rate, flame surface density, and scalar dissipation rate in a weakly turbulent premixed flame, Combust. Theory Modelling 23 (2) (2019) 245–260.
[113] R. Yu, A. N. Lipatnikov, A DNS study of sensitivity of scaling exponents for premixed turbulent consumption velocity to transient effects, Flow Turbulence Combust. 102 (3) (2019) 679–698.
[114] C. Chi, G. Janiga, K. Zaehringer, D. Thevenin, DNS study of the optimal heat release rate marker in premixed methane flames, Proc. Combust. Inst. 37 (2) (2019) 2363–2371.
[115] A. Er-raiy, Z. Bouali, J. Reveillon, A. Mura, Optimized single-step (OSS) chemistry models for the simulation of turbulent premixed flame propagation, Combust. Flame 192 (2018) 130–148.
[116] D. Suckart, D. Linse, Modelling turbulent premixed flame-wall interactions including flame quenching and near-wall turbulence based on a level-set flamelet approach, Combust. Flame 190 (2018) 50–64.
[117] T. Grenga, J. F. MacArt, M. E. Mueller, Dynamic mode decomposition of a direct numerical simulation of a turbulent premixed planar jet flame: convergence of the modes, Combust. Theory Modelling 22 (4) (2018) 795–811.
[118] A. Attili, S. Luca, D. Denker, F. Bisetti, H. Pitsch, Turbulent flame speed and reaction layer thickening in premixed jet flames at constant karlovitz and increasing reynolds numbers, Proc. Combust. Inst. 38 (2) (2021) 2939–2947.
[119] Q. Male, O. Vermorel, F. Ravet, T. Poinsot, Direct numerical simulations and models for hot burnt gases jet ignition, Combust. Flame 223 (2021) 407–422.
[120] A. N. Lipatnikov, V. A. Sabelnikov, F. E. Hernandez-Perez, W. Song, H. G. Im, A priori DNS study of applicability of flamelet concept to predicting

mean concentrations of species in turbulent premixed flames at various Karlovitz numbers, Combust. Flame 222 (2020) 370–382.
[121] D. Dasgupta, W. Sun, M. Day, A. J. Aspden, T. Lieuwen, Analysis of chemical pathways and flame structure for n-dodecane/air turbulent premixed flames, Combust. Flame 207 (2019).
[122] R. Yu, A. N. Lipatnikov, Statistics conditioned to isoscalar surfaces in highly turbulent premixed reacting systems, Comput. Fluids 187 (2019) 69–82.
[123] A. J. Aspden, N. Zettervall, C. Fureby, An a priori analysis of a DNS database of turbulent lean premixed methane flames for LES with finite-rate chemistry, Proc. Combust. Inst. 37 (2) (2019) 2601–2609.
[124] S. Trivedi, G. V. Nivarti, R. S. Cant, Flame self-interactions with increasing turbulence intensity, Proc. Combust. Inst. 37 (2) (2019) 2443–2449.
[125] M. Klein, C. Kasten, N. Chakraborty, A-priori Direct Numerical Simulation assessment of models for generalized sub-grid scale turbulent kinetic energy in turbulent premixed flames, Comput. Fluids 154 (2017) 123–131.
[126] K. Aoki, M. Shimura, Y. Naka, M. Tanahashi, Disturbance energy budget of turbulent swirling premixed flame in a cuboid combustor, Proc. Combust. Inst. 36 (3) (2017) 3809–3816.
[127] A. N. Lipatnikov, V. A. Sabelnikov, F. E. Hernandez-Perez, W. Song, H. G. Im, Prediction of mean radical concentrations in lean hydrogen-air turbulent flames at different karlovitz numbers adopting a newly extended flamelet-based presumed PDF, Combust. Flame 226 (2021) 248–259.
[128] M. Pfitzner, M. Klein, A near-exact analytic solution of progress variable and pdf for single-step Arrhenius chemistry, Combust. Flame 226 (2021) 380–395.
[129] A. N. Lipatnikov, V. A. Sabelnikov, Evaluation of mean species mass fractions in premixed turbulent flames: A DNS study, Proc. Combust. Inst. 38 (4) (2021) 6413–6420.
[130] R. Rasool, N. Chakraborty, M. Klein, Effect of non-ambient pressure conditions and lewis number variation on direct numerical simulation of turbulent bunsen flames at low turbulence intensity, Combust. Flame 231 (2021).
[131] J. You, Y. Yang, Modelling of the turbulent burning velocity based on lagrangian statistics of propagating surfaces, J. Fluid Mech. 887 (2020).
[132] G. Ghiasi, N. A. K. Doan, N. Swaminathan, B. Yenerdag, Y. Minamoto, M. Tanahashi, Assessment of SGS closure for isochoric combustion of hydrogen-air mixture, Int. J. Hydrogen Energy 43 (16) (2018) 8105–8115.
[133] L. Tian, R. P. Lindstedt, The impact of dilatation, scrambling, and pressure transport in turbulent premixed flames, Combust. Theory Modelling 21 (6) (2017) 1114–1147.
[134] A. Herbert, U. Ahmed, N. Chakraborty, M. Klein, Applicability of extrapolation relations for curvature and stretch rate dependences of displacement speed for statistically planar turbulent premixed flames, Combust. Theory Modelling 24 (6) (2020) 1021–1038.
[135] T. Falkenstein, S. Kang, L. Cai, M. Bode, H. Pitsch, DNS study of the global heat release rate during early flame kernel development under engine conditions, Combust. Flame 213 (2020) 455–466.
[136] V. Papapostolou, N. Chakraborty, M. Klein, H. G. Im, Statistics of scalar flux transport of major species in different premixed turbulent combustion regimes for H-2-air flames, Flow Turbulence Combust. 102 (4) (2019) 931–955.
[137] H. Wang, Z. Wang, K. Luo, E. R. Hawkes, J. H. Chen, J. Fan, Direct numerical simulation of turbulent boundary layer premixed combustion under autoignitive conditions, Combust. Flame 228 (2021) 292–301.
[138] S. Benekos, C. E. Frouzakis, G. K. Giannakopoulos, C. Altantzis, K. Boulouchos, A 2-D DNS study of the effects of nozzle geometry, ignition kernel placement and initial turbulence on prechamber ignition, Combust. Flame 225 (2021) 272–290.
[139] J. Ren, H. Wang, G. Chen, K. Luo, J. Fan, Predictive models for flame evolution using machine learning: A priori assessment in turbulent flames without and with mean shear, Phys. Fluids 33 (5) (2021).
[140] S. Yellapantula, B. A. Perry, R. W. Grout, Deep learning-based model for progress variable dissipation rate in turbulent premixed flames, Proc. Combust. Inst. 38 (2) (2021) 2929–2938.
[141] J. Lee, J. F. MacArt, M. E. Mueller, Heat release effects on the reynolds stress budgets in turbulent premixed jet flames at low and high Karlovitz numbers, Combust. Flame 216 (2020) 1–8.
[142] A. N. Lipatnikov, V. A. Sabelnikov, N. V. Nikitin, S. Nishiki, T. Hasegawa, Influence of thermal expansion on potential and rotational components of turbulent velocity field within and upstream of premixed flame brush, Flow Turbulence Combust. 106 (4) (2021) 1111–1124.
[143] F. B. Keil, M. Klein, N. Chakraborty, Sub-grid reaction progress variable variance closure in turbulent premixed flames, Flow Turbulence Combust. 106 (4) (2021) 1195–1212.
[144] R. Yu, T. Nilsson, G. Brethouwer, N. Chakraborty, A. Lipatnikov, Assessment of an evolution equation for the displacement speed of a constant-density reactive scalar field, Flow Turbulence Combust. 106 (4) (2021) 1091–1110.
[145] X. Zhao, Y. Tao, T. Lu, H. Wang, Sensitivities of direct numerical simulations to chemical kinetic uncertainties: spherical flame kernel evolution of a real jet fuel, Combust. Flame 209 (2019) 117–132.
[146] C. Chi, G. Janiga, D. Thevenin, On-the-fly artificial neural network for chemical kinetics in direct numerical simulations of premixed combustion, Combust. Flame 226 (2021) 467–477.
[147] F. Ladeinde, H. Oh, Stochastic and spectra contents of detonation initiated by compressible turbulent thermodynamic fluctuations, Phys. Fluids 33 (4) (2021).
[148] A. Krisman, P. Meagher, X. Zhao, J.-W. Park, T. Lu, J. H. Chen, A direct numerical simulation of jet A flame kernel quenching, Combust. Flame 225 (2021) 349–363.
[149] P. Zhao, L. Wang, N. Chakraborty, Effects of the cold wall boundary on the flame structure and flame speed in premixed turbulent combustion, Proc. Combust. Inst. 38 (2) (2021) 2967–2976.
[150] M.-C. Ma, M. Talei, R. D. Sandberg, Direct numerical simulation of turbulent premixed jet flames: Influence of inflow boundary conditions, Combust. Flame 213 (2020) 240–254.
[151] J. A. M. Medina, H. Schmidt, F. Mauss, Z. Jozefik, Constant volume n-heptane autoignition using One-Dimensional Turbulence, Combust. Flame 190

(2018) 388–401.
[152] S. Berger, F. Duchaine, L. Y. M. Gicquel, Bluff-body thermal property and initial state effects on a laminar premixed flame anchoring pattern, Flow Turbulence Combust. 100 (2) (2018) 561–591.
[153] U. Ahmed, A. Herbert, N. Chakraborty, M. Klein, On the validity of Damkohler's second hypothesis in statistically planar turbulent premixed flames in the thin reaction zones regime, Proc. Combust. Inst. 38 (2) (2021) 3039–3047.
[154] W. Song, F. E. H. Perez, E.-A. Tingas, H. G. Im, Statistics of local and global flame speed and structure for highly turbulent H-2/air premixed flames, Combust. Flame 232 (2021).
[155] P. Pouech, F. Duchaine, T. Poinsot, Premixed flame ignition in high-speed flows over a backward facing step, Combust. Flame 229 (2021).
[156] A. N. Lipatnikov, T. Nilsson, R. Yu, X. S. Bai, V. A. Sabelnikov, Assessment of a flamelet approach to evaluating mean species mass fractions in moderately and highly turbulent premixed flames, Phys. Fluids 33 (4) (2021).
[157] Y. G. Shah, J. G. Brasseur, Y. Xuan, An a priori analysis of the structure of local subfilter-scale species surrounding flame fronts using direct numerical simulation of turbulent premixed flames, Phys. Fluids 33 (4) (2021).
[158] H. Wang, E. R. Hawkes, J. Ren, G. Chen, K. Luo, J. Fan, 2-D and 3-D measurements of flame stretch and turbulence-flame interactions in turbulent premixed flames using DNS, J. Fluid Mech. 913 (2021).
[159] J. R. Bailey, E. S. Richardson, DNS analysis of boundary layer flashback in turbulent flow with wall-normal pressure gradient, Proc. Combust. Inst. 38 (2) (2021) 2791–2799.
[160] Z. Lu, Y. Yang, Modeling pressure effects on the turbulent burning velocity for lean hydrogen/air premixed combustion, Proc. Combust. Inst. 38 (2) (2021) 2901–2908.
[161] V. A. Sabelnikov, A. N. Lipatnikov, N. Nikitin, S. Nishiki, T. Hasegawa, Application of Helmholtz-Hodge decomposition and conditioned structure functions to exploring influence of premixed combustion on turbulence upstream of the flame, Proc. Combust. Inst. 38 (2) (2021) 3077–3085.
[162] H. Xiao, K. Luo, T. Jin, H. Wang, J. Fan, Direct numerical simulation of turbulence modulation by premixed flames in a model annular swirling combustor, Proc. Combust. Inst. 38 (2) (2021) 3013–3020.
[163] S. H. Kim, Y. Su, Front propagation formulation for large eddy simulation of turbulent premixed flames, Combust. Flame 220 (2020) 439–454.
[164] F. B. Keil, N. Chakraborty, M. Klein, Analysis of the closures of sub-grid scale variance of reaction progress variable for turbulent bunsen burner flames at different pressure levels, Flow Turbulence Combust. 105 (2020) 869–888.
[165] D. Kim, K. Y. Huh, Conditional relationships for the layered brush structure of turbulent premixed flames in statistical steadiness, Combust. Flame 204 (2019) 103–115.
[166] Z. M. Nikolaou, N. Swaminathan, Assessment of FSD and SDR closures for turbulent flames of alternative fuels, Flow Turbulence Combust. 101 (3) (2018) 759–774.
[167] J. Liu, H. Wang, Machine learning assisted modeling of mixing timescale for LES/PDF of high-Karlovitz turbulent premixed combustion, Combust. Flame 238 (2022).
[168] H. Shehab, H. Watanabe, Y. Minamoto, R. Kurose, T. Kitagawa, Morphology and structure of spherically propagating premixed turbulent hydrogen-air flames, Combust. Flame 238 (2022).
[169] A. Datta, J. Mathew, S. Hemchandra, The explicit filtering method for large eddy simulations of a turbulent premixed flame, Combust. Flame 237 (2022).
[170] E. Suillaud, K. Truffin, O. Colin, D. Veynante, Direct numerical simulations of high Karlovitz number premixed flames for the analysis and modeling of the displacement speed., Combust. Flame 236 (2022).
[171] H. Lee, P. Dai, M. Wan, A. N. Lipatnikov, A DNS study of extreme and leading points in lean hydrogen-air turbulent flames-Part i: Local thermochemical structure and reaction rates, Combust. Flame 235 (2022).
[172] H. Lee, P. Dai, M. Wan, A. N. Lipatnikov, A DNS study of extreme and leading points in lean hydrogen-air turbulent flames-Part ii: Local velocity field and flame topology, Combust. Flame 235 (2022).
[173] R. Nakazawa, Y. Minamoto, N. Inoue, M. Tanahashi, Species reaction rate modelling based on physics-guided machine learning, Combust. Flame 235 (2022).
[174] H. C. Lee, P. Dai, M. Wan, A. N. Lipatnikov, Influence of molecular transport on burning rate and conditioned species concentrations in highly turbulent premixed flames, J. Fluid Mech. 928 (2021).
[175] T. Ding, T. Readshaw, S. Rigopoulos, W. P. Jones, Machine learning tabulation of thermochemistry in turbulent combustion: An approach based on hybrid flamelet/random data and multiple multilayer perceptrons, Combust. Flame 231 (2021).
[176] C. Chi, A. Abdelsamie, D. Thevenin, Transient ignition of premixed methane/air mixtures by a prechamber hot jet: a DNS study, Flow Turbulence Combust. (2021).
[177] A. R. Varma, U. Ahmed, N. Chakraborty, Effects of body forces on the statistics of flame surface density and its evolution in statistically planar turbulent premixed flames, Flow Turbulence Combust. 108 (1) (2022) 181–212.
[178] S. Yang, Development of a mechanism-dynamic-selection turbulent premixed combustion model with application to gasoline engine combustion and emissions simulation, Combust. Theory Modelling 25 (2) (2021) 315–350.
[179] K. Luo, R. Liu, Y. Bai, A. Attili, H. Pitsch, F. Bisetti, J. Fan, A-priori and a-posteriori studies of a direct moment closure approach for turbulent combustion using DNS data of a premixed flame(star), Proc. Combust. Inst. 38 (2) (2021) 3003–3011.
[180] T. Falkenstein, H. Chu, M. Bode, S. Kang, H. Pitsch, The role of differential diffusion during early flame kernel development under engine conditions - Part ii: Effect of flame structure and geometry, Combust. Flame 221 (2020) 516–529.
[181] K. G. Bhide, S. Sreedhara, A DNS study on turbulence-chemistry interaction in lean premixed syngas flames, Int. J. Hydrogen Energy 45 (43) (2020) 23615–23623.
[182] R. Schiessl, J. A. Denev, DNS-studies on flame front markers for turbulent premixed combustion, Combust. Theory Modelling 24 (6) (2020) 983–1001.
[183] K. Aoki, M. Shimura, J. Park, Y. Minamoto, M. Tana-

hashi, Response of heat release rate to flame straining in swirling hydrogen-air premixed flames, Flow Turbulence Combust. 104 (2-3) (2020) 451–478.
[184] A. Haghiri, M. Talei, M. J. Brear, E. R. Hawkes, Flame annihilation displacement speed and stretch rate in turbulent premixed flames, Flow Turbulence Combust. 104 (4) (2020) 977–996.
[185] S. Zhang, Z. Lu, Y. Yang, Modeling the displacement speed in the flame surface density method for turbulent premixed flames at high pressures, Phys. Fluids 33 (4) (2021).
[186] J. Ren, H. Wang, K. Luo, J. Fan, A priori assessment of convolutional neural network and algebraic models for flame surface density of high Karlovitz premixed flames, Phys. Fluids 33 (3) (2021).
[187] P. Zhang, T. Xie, H. Kolla, H. Wang, E. R. Hawkes, J. H. Chen, H. Wang, A priori analysis of a power-law mixing model for transported PDF model based on high Karlovitz turbulent premixed dns flames, Proc. Combust. Inst. 38 (2) (2021) 2917–2927.
[188] R. Rasool, N. Chakraborty, M. Klein, Algebraic flame surface density modelling of high pressure turbulent premixed Bunsen flames, Flow Turbulence Combust. 106 (4) (2021) 1313–1327.
[189] U. Ahmed, N. Chakraborty, M. Klein, Assessment of Bray Moss Libby formulation for premixed flame-wall interaction within turbulent boundary layers: Influence of flow configuration, Combust. Flame 233 (2021).
[190] T. Nilsson, I. Langella, N. A. K. Doan, N. Swaminathan, R. Yu, X.-S. Bai, A priori analysis of sub-grid variance of a reactive scalar using DNS data of high Ka flames, Combust. Theory Modelling 23 (5) (2019) 885–906.
[191] M. Akram, V. Raman, Using approximate inertial manifold approach to model turbulent non-premixed combustion, Phys. Fluids 33 (3) (2021).
[192] J. An, G. He, F. Qin, X. Wei, B. Liu, Dynamic adaptive chemistry with mechanisms tabulation and in situ adaptive tabulation (ISAT) for computationally efficient modeling of turbulent combustion, Combust. Flame 206 (2019) 467–475.
[193] W. L. Chan, M. Ihme, Flamelet regime characterization for non-premixed turbulent combustion simulations, Combust. Flame 186 (2017) 220–235.
[194] C. Han, H. Wang, Effect of unsteadiness and scalar dissipation models on flamelet modeling of differential molecular diffusion in turbulent non-premixed DNS flames, Flow Turbulence Combust. (2022).
[195] Z. X. Chen, N. A. K. Doan, S. Ruan, I. Langella, N. Swaminathan, Apriori investigation of subgrid correlation of mixture fraction and progress variable in partially premixed flames, Combust. Theory Modelling 22 (5) (2018) 862–882.
[196] G. Chen, H. Wang, K. Luo, J. Fan, Flame edge structures and dynamics in planar turbulent non-premixed inclined slot-jet flames impinging at a wall, J. Fluid Mech. 920 (2021).
[197] S. Chevillard, J.-B. Michel, C. Pera, J. Reveillon, Evaluation of different turbulent combustion models based on tabulated chemistry using DNS of heterogeneous mixtures, Combust. Theory Modelling 21 (3) (2017) 440–465.
[198] F. C. Cunha Galeazzo, B. Savard, H. Wang, E. R. Hawkes, J. H. Chen, G. C. Krieger Filho, Performance assessment of flamelet models in flame-resolved LES of a high Karlovitz methane/air stratified premixed jet flame, Proc. Combust. Inst. 37 (2) (2019) 2545–2553.
[199] D. Denker, A. Attili, M. Gauding, K. Niemietz, M. Bode, H. Pitsch, A new modeling approach for mixture fraction statistics based on dissipation elements, Proc. Combust. Inst. 38 (2) (2021) 2681–2689.
[200] N. A. K. Doan, S. Bansude, K. Osawa, Y. Minamoto, T. Lu, J. H. Chen, N. Swaminathan, Identification of combustion mode under MILD conditions using chemical explosive mode analysis, Proc. Combust. Inst. 38 (4) (2021) 5415–5422.
[201] M. Gauding, M. Bode, D. Denker, Y. Brahami, L. Danaila, E. Varea, On the combined effect of internal and external intermittency in turbulent non-premixed jet flames, Proc. Combust. Inst. 38 (2) (2021) 2767–2774.
[202] M. U. Goktolga, L. P. H. de Goey, J. A. van Oijen, Modeling curvature effects in turbulent autoigniting non-premixed flames using tabulated chemistry, Proc. Combust. Inst. 38 (2) (2021) 2741–2748.
[203] E. Gorgoraptis, J.-B. Michel, S. Chevillard, A. P. da Cruz, Evaluation of different turbulent combustion models based on tabulated chemistry using DNS of heterogeneous mixtures under multi-injection diesel engine-relevant conditions, Flow Turbulence Combust. 107 (2) (2021) 479–515.
[204] C. Han, D. O. Lignell, E. R. Hawkes, J. H. Chen, H. Wang, Examination of the effect of differential molecular diffusion in DNS of turbulent non-premixed flames, Int. J. Hydrogen Energy 42 (16) (2017) 11879–11892.
[205] S. Hartl, D. Geyer, C. Hasse, X. Zhao, H. Wang, R. S. Barlow, Assessing an experimental approach for chemical explosive mode and heat release rate using DNS data, Combust. Flame 209 (2019) 214–224.
[206] E. Illana, D. Mira, A. Mura, An extended flame index partitioning for partially premixed combustion, Combust. Theory Modelling 25 (1) (2021) 121–157.
[207] E. Inanc, A. M. Kempf, N. Chakraborty, Scalar gradient and flame propagation statistics of a flame-resolved laboratory-scale turbulent stratified burner simulation, Combust. Flame 238 (2022).
[208] T. Jin, C. Song, H. Wang, Z. Gao, K. Luo, J. Fan, Direct numerical simulation of a supercritical hydrothermal flame in a turbulent jet, J. Fluid Mech. 922 (2021).
[209] K. S. Jung, S. O. Kim, T. Lu, J. H. Chen, C. S. Yoo, On the flame stabilization of turbulent lifted hydrogen jet flames in heated coflows near the autoignition limit: A comparative DNS study, Combust. Flame 233 (2021).
[210] A. H. Mahdipour, M. M. Salehi, Localized conditional source-term estimation model for turbulent combustion, Combust. Flame 235 (2022).
[211] N. A. K. Doan, N. Swaminathan, Y. Minamoto, DNS of MILD combustion with mixture fraction variations, Combust. Flame 189 (2018) 173–189.
[212] A. Shamooni, A. Cuoci, T. Faravelli, A. Sadiki, New dynamic scale similarity based finite-rate combustion models for LES and a priori DNS assessment in non-premixed jet flames with high level of local extinction, Flow Turbulence Combust. 104 (1) (2020) 233–260.
[213] A. Shamooni, A. Cuoci, T. Faravelli, A. Sadiki, An a priori DNS analysis of scale similarity based combustion models for LES of non-premixed jet flames,

Flow Turbulence Combust. 104 (2-3) (2020) 605–624.

[214] A. Validi, H. Schock, F. Jaberi, Turbulence-combustion interactions in premixed and non-premixed flames generated by hot active turbulent jets, Flow Turbulence Combust. 106 (3) (2021) 849–880.

[215] K. Wan, C. Barnaud, L. Vervisch, P. Domingo, Chemistry reduction using machine learning trained from non-premixed micro-mixing modeling: Application to DNS of a syngas turbulent oxy-flame with side-wall effects, Combust. Flame 220 (2020) 119–129.

[216] K. Wan, C. Barnaud, L. Vervisch, P. Domingo, Machine learning for detailed chemistry reduction in DNS of a syngas turbulent oxy-flame with side-wall effects, Proc. Combust. Inst. 38 (2) (2021) 2825–2833.

[217] H. Wang, G. Chen, K. Luo, E. R. Hawkes, J. H. Chen, J. Fan, Turbulence/flame/wall interactions in non-premixed inclined slot-jet flames impinging at a wall using direct numerical simulation, Proc. Combust. Inst. 38 (2) (2021) 2711–2720.

[218] T. Yao, W. H. Yang, K. H. Luo, Direct numerical simulation study of hydrogen/air auto-ignition in turbulent mixing layer at elevated pressures, Comput. Fluids 173 (2018) 59–72.

[219] T. Zirwes, F. Zhang, P. Habisreuther, M. Hansinger, H. Bockhorn, M. Pfitzner, D. Trimis, Quasi-Dns dataset of a piloted flame with inhomogeneous inlet conditions, Flow Turbulence Combust. 104 (4) (2020) 997–1027.

[220] H. Wang, E. R. Hawkes, B. Savard, J. H. Chen, Direct numerical simulation of a high Ka CH4/air stratified premixed jet flame, Combust. Flame 193 (2018) 229–245.

[221] W. K. Bushe, C. Devaud, J. Bellan, A priori evaluation of the double-conditioned conditional source-term estimation model for high-pressure heptane turbulent combustion using DNS data obtained with one-step chemistry, Combust. Flame 217 (2020) 131–151.

[222] K. Jigjid, C. Tamaoki, Y. Minamoto, R. Nakazawa, N. Inoue, M. Tanahashi, Data driven analysis and prediction of MILD combustion mode, Combust. Flame 223 (2021) 474–485.

[223] C. Turquand d'Auzay, N. Chakraborty, The localised forced ignition and early stages of flame development in a turbulent planar jet, Proc. Combust. Inst. 38 (2) (2021) 2775–2782.

[224] K. Aditya, A. Gruber, C. Xu, T. Lu, A. Krisman, M. R. Bothien, J. H. Chen, Direct numerical simulation of flame stabilization assisted by autoignition in a reheat gas turbine combustor, Proc. Combust. Inst. 37 (2) (2019) 2635–2642.

[225] B. O. Arani, C. E. Frouzakis, J. Mantzaras, K. Boulouchos, Three-dimensional direct numerical simulations of turbulent Fuel-lean H-2/air hetero-/homogeneous combustion over Pt with detailed chemistry, Proc. Combust. Inst. 36 (3) (2017) 4355–4363.

[226] J. R. Bailey, E. S. Richardson, DNS analysis of boundary layer flashback in turbulent flow with wall-normal pressure gradient, Proc. Combust. Inst. 38 (2) (2021) 2791–2799.

[227] A. Gruber, M. R. Bothien, A. Ciani, K. Aditya, J. H. Chen, F. A. Williams, Direct numerical simulation of hydrogen combustion at auto-ignitive conditions: Ignition, stability and turbulent reaction-front velocity, Combust. Flame 229 (2021).

[228] H. Shehab, H. Watanabe, Y. Minamoto, R. Kurose, T. Kitagawa, Morphology and structure of spherically propagating premixed turbulent hydrogen-air flames, Combust. Flame 238 (2022).

[229] T. Yao, Q. Wang, K. H. Luo, Formation and evolution of flame kernels in autoignition of a turbulent hydrogen/air mixing layer at 50 atm, Fuel 255 (2019).

[230] J. J. Behzadi, M. Talei, M. Bolla, E. R. Hawkes, T. Lucchini, G. D'Errico, S. Kook, A conditional moment closure study of chemical reaction source terms in SCCI combustion, Flow Turbulence Combust. 100 (1) (2018) 93–118.

[231] A. Krisman, P. Meagher, X. Zhao, J.-W. Park, T. Lu, J. H. Chen, A direct numerical simulation of jet A flame kernel quenching, Combust. Flame 225 (2021) 349–363.

[232] P. L. K. Paes, Y. Xuan, Numerical investigation of turbulent kinetic energy dynamics in chemically-reacting homogeneous turbulence, Flow Turbulence Combust. 101 (3) (2018) 775–794.

[233] K. Bardis, P. Kyrtatos, C. E. Frouzakis, Y. M. Wright, G. K. Giannakopoulos, K. Boulouchos, Reduction of RANS/LES combustion sub-models for quasi-dimensional spark ignition engine simulations and evaluation of the modelling assumptions with DNS, Combust. Flame 220 (2020) 189–202.

[234] M. T. H. de Frahan, S. Yellapantula, R. King, M. S. Day, R. W. Grout, Deep learning for presumed probability density function models, Combust. Flame 208 (2019) 436–450.

[235] C. Mandanis, M. Schmitt, J. Koch, Y. M. Wright, K. Boulouchos, Wall heat flux and thermal stratification investigations during the compression stroke of an engine-like geometry: A comparison between LES and DNS, Flow Turbulence Combust. 100 (3) (2018) 769–795.

[236] P. P. Popov, Alternatives to the beta distribution in assumed PDF methods for turbulent reactive flow, Flow Turbulence Combust. 108 (2022) 433459.

[237] Y. G. Shah, J. G. Brasseur, Y. Xuan, Assessment of disparities in estimating filtered chemical reaction rates in LES using DNS of turbulent premixed flames, Combust. Theory Modelling 24 (6) (2020) 1179–1194.

[238] SENGA description, `https://www.ukctrf.com/index.php/senga/` (2021).

[239] J. H. Chen, A. Choudhary, B. De Supinski, M. DeVries, E. R. Hawkes, S. Klasky, W.-K. Liao, K.-L. Ma, J. Mellor-Crummey, N. Podhorszki, et al., Terascale direct numerical simulations of turbulent combustion using S3D, Comput. Sci. Disc. 2 (1) (2009) 015001.

[240] A. Abdelsamie, G. Fru, T. Oster, F. Dietzsch, G. Janiga, D. Thévenin, Towards direct numerical simulations of low-mach number turbulent reacting and two-phase flows using immersed boundaries, Comput. Fluids 131 (123) (2016).

[241] P. Kurose, FK^3 description, `http://www.tse.me.kyoto-u.ac.jp/members/kurose/link_e.php` (2021).

[242] F. E. Hernández Pérez, N. Mukhadiyev, X. Xu, A. Sow, B. J. Lee, R. Sankaran, H. G. Im, Direct numerical simulations of reacting flows with detailed chemistry using many-core/GPU acceleration, Comput. Fluids 173 (2018) 73–79.

[243] M. Pettit, B. Coriton, A. Gomez, A. Kempf, Large-eddy simulation and experiments on non-premixed highly turbulent opposed jet flows, Proc. Combust. Inst. 33 (2011) 1391–1399.
[244] E. Motheau, J. Abraham, A high-order numerical algorithm for DNS of low-Mach-number reactive flows with detailed chemistry and quasi-spectral accuracy, J. Comput. Physics 313 (15) (2008) 7125–7159.
[245] O. Desjardins, G. Blanquart, G. Balarac, H. Pitsch, High order conservative finite difference scheme for variable density low Mach number turbulent flow, J. Comput. Phys. 15 (2016) 430–454.
[246] AVBP description, http://www.cerfacs.fr/avbp7x/ (2021).
[247] P. Fischer, J. Lottes, S. Kerkemeier, Nek5000 description, http://nek5000.mcs.anl.gov (2021).
[248] OpenFoam description, https://www.openfoam.com (2021).
[249] P. Moin, K. Mahesh, Direct numerical simulation: A tool in turbulence research, Annu. Rev. Fluid Mech. 30 (1998) 539–578.
[250] W. Meier, P. Weigand, X. Duan, R. Giezendanner-Thoben, Detailed characterization of the dynamics of thermoacoustic pulsations in a lean premixed swirl flame, Combust. Flame 150 (1/2) (2007) 2–26.
[251] R. Borghi, Turbulent combustion modelling, Prog. Energy Combust. Sci. 14 (1988) 245–292.
[252] P. Domingo, L. Vervisch, Revisiting the relation between premixed flame brush thickness and turbulent burning velocities from Ken Bray's notes, Combust. Flame 239 (111706) (2022).
[253] N. Peters, Turbulent Combustion, Cambridge University Press, 2000.
[254] E. Knudsen, O. Kurenkov, S. Kim, M. Oberlack, H. Pitsch, Modeling flame brush thickness in premixed turbulent combustion, in: Proceedings of the Summer Program, Center for Turbulence Research, Stanford University, 2006, pp. 299–310.
[255] Y.-C. Chen, N. Peters, G. A. Schneemann, N. Wruck, U. Renz, M. S. Mansour, The detailed flame structure of highly stretched turbulent premixed methane-air flames, Combust. Flame 107 (3) (1996) 223–244.
[256] G. P. Smith, D. M. Golden, M. Frenklach, N. W. Moriarty, B. Eiteneer, M. Goldenberg, C. T. Bowman, R. K. Hanson, S. Song, W. C. Gardiner, V. V. Lissianski, Z. Qin, Gri-3.0, Tech. rep., Berkeley U., http://combustion.berkeley.edu/gri-mech/version30/text30.html (1999).
[257] G. Godel, P. Domingo, L. Vervisch, Tabulation of NOx chemistry for large-eddy simulation of non-premixed turbulent flames, Proc. Combust. Inst. 32 (2009) 1555–1561.
[258] P. Domingo, L. Vervisch, D. Veynante, Large-eddy simulation of a lifted methane jet flame in a vitiated coflow, Combust. Flame 152 (2008) 415–432.
[259] A. W. Vreman, An eddy-viscosity subgrid-scale model for turbulent shear flow: Algebraic theory and applications, Phys. Fluids. 16 (2004) 3670–3681.
[260] L. Cifuentes, C. Dopazo, J. Martin, P. Domingo, L. Vervisch, Local volumetric dilatation rate and scalar geometries in a premixed methane-air turbulent jet flame, Proc. Combust. Inst. 35 (2) (2015) 1295–1303.
[261] C. Dopazo, E. O'Brien, Functional formulation of nonisothermal turbulent reactive flows, Phys. Fluids 17 (1974) 1968–1975.
[262] Z. Nikolaou, L. Vervisch, A priori assessment of an iterative deconvolution method for LES sub-grid scale variance modelling, Flow Turbulence Combust. 101 (1) (2018) 33–53.
[263] Z. Nikolaou, R. S. Cant, L. Vervisch, Scalar flux modelling in turbulent flames using iterative deconvolution, Phys. Rev. Fluids. 3 (4) (2018) 043201.
[264] Z. Nikolaou, C. Chrysostomou, L. Vervisch, R. S. Cant, Progress variable variance and filtered rate modelling using convolutional neural networks and flamelet methods, Flow Turbulence Combust. 103 (2) (2019) 485–501.
[265] Z. M. Nikolaou, Y. Minamoto, L. Vervisch, Unresolved stress tensor modelling in turbulent premixed v-flames using iterative deconvolution: An a priori assessment, Phys. Rev. Fluids. 4 (6) (2019) 063202.
[266] Q. Wang, M. Ihme, Regularized deconvolution method for turbulent combustion modeling, Combust. Flame 176 (2017).
[267] A. Seltz, P. Domingo, L. Vervisch, Z. M. Nikolaou, Direct mapping from LES resolved scales to filtered-flame generated manifolds using convolutional neural networks, Combust. Flame 210 (2019) 71–82.
[268] P. Domingo, L. Vervisch, Large Eddy Simulation of premixed turbulent combustion using approximate deconvolution and explicit flame filtering, Proc. Combust. Inst. 35 (2) (2015) 1349–1357.
[269] K. N. C. Bray, The challenge of turbulent combustion, Symp. (Int.) on Combust. 26 (1996) 1–26.
[270] M. S. Sweeney, S. Hochgreb, M. J. Dunn, R. S. Barlow, The structure of turbulent stratified and premixed methane/air flames {I}: Non-swirling flows, Combust. Flame 159 (9) (2012) 2896 – 2911.
[271] R. Zhou, S. Balusamy, M. S. Sweeney, R. S. Barlow, S. Hochgreb, Flow field measurements of a series of turbulent premixed and stratified methane/air flames, Combust. Flame 160 (10) (2013) 2017 – 2028.
[272] N. Peters, Multiscale combustion and turbulence, Proc. Combust. Inst. 32 (1) (2009) 1–25.
[273] R. Ranade, T. Echekki, A framework for data-based turbulent combustion closure: A posteriori validation, Combust. Flame 210 (2019) 279–291.
[274] O. Owoyele, P. Kundu, M. M. Ameen, T. Echekki, S. Som, Application of deep artificial neural networks to multi-dimensional flamelet libraries and spray flames, Int. J. Eng. Research 21 (1) (2020) 151–168.
[275] Z. M. Nikolaou, C. Chrysostomou, Y. Minamoto, L. Vervisch, Evaluation of a neural network-based closure for the unresolved stresses in turbulent premixed V-flames, Flow Turbulence Combust. 106 (2) (2021) 331?356.
[276] G. Lodier, C. Merlin, P. Domingo, L. Vervisch, F. Ravet, Self-ignition scenarios after rapid compression of a turbulent mixture weakly-stratified in temperature, Combust. Flame 159 (11) (2012) 3358–3371.
[277] V. Moureau, P. Domingo, L. Vervisch, Design of a massively parallel CFD code for complex geometries, C.R. Mecanique 339 (2011) 141–148.
[278] C. Locci, L. Vervisch, B. Farcy, N. Perret, Selective non-catalytic reduction (SNCR) of nitrogen oxide emissions: A perspective from numerical modeling, Flow Turbulence Combust. 100 (2) (2018) 301–340.
[279] G. Lodier, P. Domingo, L. Vervisch, Quantification of the pre-ignition front propagation in DNS of rapidly compressed mixture, Flow Turbulence Com-

bust. 94 (1) (2015) 219–235.
[280] F. B. Keil, M. Amzehnhoff, U. Ahmed, N. Chakraborty, M. Klein, Comparison of flame propagation statistics extracted from direct numerical simulation based on simple and detailed chemistry-part 1: Fundamental flame turbulence interaction, Energies 14 (5548) (2021).
[281] L. Lannelongue, J. Grealey, I. M., Green algorithms: Quantifying the carbon footprint of computation, Advance Sciences 8 (12) (2021).
[282] How green are your computations?, http://www.green-algorithms.org (2021).
[283] F. Berthoud, B. Bzeznik, N. Nicolas Gibelin, M. Laurens, C. Bonamy, M. Morel, S. X., Estimation de l'empreinte carbone d'une heure.coeur de calcul., Tech. rep., INRIA (2020).
[284] M. Raissi, P. Perdikaris, G. Karniadakis, Physics-informed neural networks: A deep learning framework for solving forward and inverse problems involving nonlinear partial differential equations, J. Comput. Phys. 378 (2019) 686–707.